UNITED
TECHNOLOGIES
RESEARCH
CENTER

East Hartford, Connecticut 06108

R94-970439-2

The Environmental Durability of Fiber Reinforced Ceramic Matrix Composites

ANNUAL REPORT

Contract N00014-93-C-0065

REPORTED BY _____
J. J. Brennan

APPROVED BY _____
K. M. Prewo, Manager of
Materials Sciences

DATE: 8/15/94

REPORT DOCUMENTATION PAGE

Form Approved
OMB No. 0704-0188

1. AGENCY USE ONLY (Leave blank)	2. REPORT DATE	3. REPORT TYPE AND DATES COVERED
	15 August 1994	Annual Report 7/6/93-7/6/94

4. TITLE AND SUBTITLE

THE ENVIRONMENTAL DURABILITY OF FIBER REINFORCED CERAMIC MATRIX COMPOSITES

5. FUNDING NUMBERS

N00014-93-C-0065

6. AUTHOR(S)

J. J. Brennan

7. PERFORMING ORGANIZATION NAME(S) AND ADDRESS(ES)

United Technologies Research Center
411 Silver Lane
East Hartford, CT 06108

8. PERFORMING ORGANIZATION REPORT NUMBER

R94-970439-2

9. SPONSORING/MONITORING AGENCY NAME(S) AND ADDRESS(ES)

Dr.S. G. Fishman, Code 1131N
Department of the Navy
Office of Naval Research
800 N. Quincy Street
Arlington, VA 22217-5000

10. SPONSORING/MONITORING AGENCY REPORT NUMBER

11. SUPPLEMENTARY NOTES

12a. DISTRIBUTION/AVAILABILITY STATEMENT

DISTRIBUTION: UNLIMITED.

12b. DISTRIBUTION CODE

13. ABSTRACT *(Maximum 200 words)*

The main objective of this program is to investigate the environmental durability of ceramic matrix composites based on glass-ceramic and polymer pyrolysis matrices, with emphasis on the relationship between composite properties, microstructure, and chemistry, and the environment to which the composite is exposed. This environmental exposure will include the effect of oxidation, moisture, and corrosion, under conditions of high temperature and stresses. During the first year of the program, the composite system under study consisted of a barium-magnesium aluminosilicate (BMAS) glass-ceramic matrix reinforced with SiC/BN coated Nicalon SiC fibers. The results of these environmental durability tests on this composite system are discussed.

14. SUBJECT TERMS

Glass-ceramic matrix composites, environmental durability of SiC/BN coated Nicalon fiber/BMAS matrix composites, corrosion of glass-ceramic matrix composites, oxidation and moisture effects on glass-ceramic matrix composites

15. NUMBER OF PAGES

59

16. PRICE CODE

17. SECURITY CLASSIFICATION OF REPORT	18. SECURITY CLASSIFICATION OF THIS PAGE	19. SECURITY CLASSIFICATION OF ABSTRACT	20. LIMITATION OF ABSTRACT
Unclassified	Unclassified	Unclassified	SAR

UNITED
TECHNOLOGIES
RESEARCH
CENTER

East Hartford, Connecticut 06108

R94-970439-2

The Environmental Durability of Fiber Reinforced Ceramic Matrix Composites

ANNUAL REPORT

Contract N00014-93-C-0065

REPORTED BY _____
J. J. Brennan

APPROVED BY _____
K. M. Prewo, Manager of
Materials Sciences

DATE: 8/15/94

TABLE OF CONTENTS

THE ENVIRONMENTAL DURABILITY OF FIBER REINFORCED CERAMIC MATRIX COMPOSITES

SUMMARY

The main objective of this program is to investigate the environmental durability of ceramic matrix composites based on glass-ceramic and polymer pyrolysis matrices, with emphasis on the relationship between composite properties, microstructure, and chemistry, and the environment to which the composite is exposed. This environmental exposure will include the effect of oxidation, moisture, and corrosion, under conditions of high temperature and stresses. During the first year of the program, the composite system under study consisted of a barium-magnesium aluminosilicate (BMAS) glass-ceramic matrix reinforced with SiC/BN coated Nicalon SiC fibers.

From the moisture exposure testing done under this program on BMAS matrix/SiC/BN coated Nicalon fiber composites, utilizing both water and humidity/furnace cycling to 1100°C, with both as-fabricated and pre-stressed composites, no degradation in composite flexural properties were found. It appears that the interfacial coating system utilized in the present composite system, CVD SiC over BN, is quite resistant to moisture and humidity, even when it is exposed to these environments due to microcracks introduced into the normally dense BMAS glass-ceramic matrix.

From the flowing oxygen exposures performed on the BMAS matrix/SiC/BN coated Nicalon fiber composites at 900°, 1000°, and 1100°C, for times of up to 100 hrs, it was found that no decrease in flexural strength, elastic modulus, or strain-to-failure of these composites occurred as a result of these exposure conditions. No significant changes were found in the composite microstructure as a result of these oxidative exposures.

For samples coated with sodium sulfate, and then exposed at temperatures of 900°-1000°C in flowing oxygen, degradation of mechanical properties and reactions in the near-surface region of the composite were found to occur. The flexural strength of the composites at RT, 1100°, and 1200°C decreased from 15-30% for all exposure temperatures. No significant decrease was noted for the composite elastic modulus or strain-to-failure, however. The short-time tensile strength at 1100°C of the composite coated with sodium sulfate did not decrease, however, a sample tested in stepped tensile stress-rupture at 1100°C did show a significant drop in ultimate fracture stress and total time to failure, compared to a composite with no sodium sulfate coating.

The appearance of the surface of the composite samples that were coated with sodium sulfate and then exposed at 900°-1000°C was that of a glassy, bubbly scale, with the amount of visible bubbling generally increasing with temperature. From surface analysis techniques including electron microprobe, scanning Auger, X-ray diffraction, and ESCA, it was found that the sample surface consisted of a sodium containing glassy phase plus crystals of magnesium silicate (enstatite) and barium aluminosilicate (celsian). Sub-surface microprobe and TEM analysis of polished composite cross-sections and TEM thin foils verified that the BMAS matrix had reacted to form a sodium containing glassy phase plus enstatite and celsian. The BN fiber coating appeared to be selectively attacked by the sodium containing glassy phase. A possible reaction sequence could be that the Nicalon fibers that are exposed to the surface oxygen are oxidized to silica, with the sodium sulfate then reacting with the crystalline barium osumilite matrix and the silica to form crystalline celsian and enstatite, plus a silica rich sodium aluminosilicate glass and sulfur trioxide gas:

$$BaMg_2Al_6Si_9O_{30} + 2Na_2SO_4 + 7SiO_2 \Rightarrow BaAl_2Si_2O_8 + 2MgSiO_3 + 2Na_2Al_2Si_6O_{16} + 2SO_3$$

The sodium containing glassy phase then appears to further attack the BN coatings and the Nicalon fibers.

It was found that burner rig thermal fatigue testing of a BMAS matrix/SiC/BN coated Nicalon fiber composite panel to a maximum of 1100°C hot-spot temperature for 6000 cycles, without the presence of sodium sulfate, did not degrade the flexural, tensile, or tensile stress-rupture properties of the composite or significantly affect the composite near-surface microstructure. However, with synthetic sea salt being continuously aspirated into the burner flame (~5ppm), the surface of the composite panel and the nickel based superalloy posts that were holding the composite in place became severely corroded, with a significant amount of glassy phase formation and the loss of 4-5 of the twelve plies of coated fibers. Even so, the composite material that was not totally corroded was not degraded in strength or toughness by the sea salt burner rig exposure.

From the results of the burner rig test conducted with synthetic sea salt, it was apparent that this exposure condition was much too severe to realistically simulate the conditions that might be encountered in a gas turbine engine. The fact that the nickel based superalloy posts were severely corroded during the test, and were not directly in the burner flame, confirms that the test conditions were not indicative of what would occur in actual gas turbine engine operation, since superalloy component corrosion of this magnitude is never experienced in the field. A more realistic test may be a cyclic test where the salt is introduced periodically by coating the burner rig

sample with synthetic sea salt, which simulates a gas turbine nozzle component that may encounter direct deposition of salt water and sea air or while the aircraft is on the ground near the ocean or on the deck of an aircraft carrier. A burner rig test of this type is recommended for future environmental testing of CMC's.

I. INTRODUCTION

During the past few years, the ceramic matrix composite (CMC) activities at UTRC have dealt primarily with the utilization of fiber coatings as a means of controlling the fiber/matrix interfacial properties in glass-ceramic matrix composites, and the investigation of polymer infiltration and pyrolysis as a method to form the matrix in fiber reinforced CMC's.

In the area of coated fiber reinforced glass-ceramic matrix composites, work both in-house at UTRC and under a current AFOSR contract has identified a coated fiber/glass-ceramic matrix composite system consisting of a barium aluminosilicate (BMAS) matrix with dual layer SiC over BN coated Nicalon fibers as having excellent strength, toughness, and oxidative stability to temperatures of ~1200°C[1,2]. The BN interfacial layer acts as a weak, crack deflecting phase, while the SiC overcoat acts as a diffusion barrier to boron diffusion from the BN into the BMAS matrix and also to matrix element diffusion into the fibers.

In addition to glass-ceramic matrix composites, UTRC has recently been involved in research into the formation of fiber reinforced ceramic composites through the polymer infiltration and pyrolysis (PIP) processing route. This type of ceramic matrix composite is more amenable to the fabrication of large, complex shapes than is the glass-ceramic matrix approach. In-house studies are dealing with the processing of Si-O-C (Blackglas) and Si_3N_4 based matrices, while contract research is concentrating on the development of novel air stable SiC precursors (AFOSR) and crystalline β-SiC precursors for the high speed civil transport (HSCT) program funded by NASA. While these programs are in their early stages compared to the glass-ceramic composite efforts, significant progress is being made such that composites processed by PIP will be introduced into the current program on CMC environmental durability during the second year of effort.

While the oxidative stability of the BMAS matrix/SiC over BN coated Nicalon fiber composites has been demonstrated to be excellent to temperatures of at least 1100°C, both unstressed and stressed, no information has been generated on the effects of actual potential engine environments that may include hot corrosion due to sulfidation, reactions due to composite to metal contact, and the effects of moisture. The PIP composites have not been thoroughly characterized under any environmental conditions, including oxidation. It is the goal of this current program to expand upon the scope of a current NAWC environmental effects program[3], and correlate the interactions that may occur in both glass-ceramic and PIP composites as a result

of the above mentioned environmental exposures with changes in composite microstructure and chemistry, in particular that associated with the fiber/coating/matrix interfacial regions. These interactions will then, in turn, be correlated to composite properties.

This report discusses the results of research activities at UTRC during the first year (July 6, 1993 - July 6, 1994) of support under this program.

II. BACKGROUND

A. Gas Turbine Engine Environment

In a gas turbine engine, components in and along the gas flow path may be exposed to high temperatures, mechanical and thermal stresses, corrodents, moisture, and oxidizing atmospheres with varying levels of oxygen and/or reducing atmospheres. In marine atmospheres experienced by many Naval aircraft, the compressor section of the engine can accumulate ultra fine sea salt particles. These salts can be chloride rich or sulfate rich[4,5], and can break loose and pass into other sections of the engine. The combustor section can generate a variety of corrodents and moisture, some caused by the ingested contaminants and some caused by the combustion process itself. Both the turbine section and the augmentor will also be affected by ingested contaminants and those produced in the combustor.

On the current NAWC contract, an in-depth study was conducted that related the environment present in different sections of a gas turbine engine to possible reactions with gas turbine components[3]. For the BMAS matrix composite material under study in this program, the environment in the combustor, turbine, and augmentor sections of military gas turbine engines are the most relevant. The following comments from the NAWC study should be considered:

Combustor

In the combustor, the dense air from the compressor is mixed with fuel and ignited. During the combustion process, up to 10% water vapor can be produced by the following reaction:

$$12N_2 + 3O_2 + 2(-CH_2-)_n \Rightarrow 12N_2 + 2CO_2 + 2H_2O \quad (1)$$

The sulfate salts that spall off compressor components pass into the combustor where they melt, vaporize, or react with water to form hydroxides. If combustion is non-stoichiometric, carbon particles may form which can act as catalysts for corrosion.

Turbine

Corrodents entering the turbine from the combustor can be in both the gaseous and condensed states. Corrodents entering with cooling air for the turbine blades from the high compressor will be in the condensed state. Those corrodents in the gaseous state will not likely cause hot corrosion, and deposition is not likely.

Augmentor

Corrodents can enter the augmentor directly from the turbine or from the low compressor through make-up air ducts. It is unlikely that salts from the combustor or from the afterburner will condense on the augmentor, and thus corrosion from this source is not likely. The main source of corrodents in the augmentor will be sea salt particles carried in with the air from the low compressor. Another source of corrosion could also be the direct deposition of salt water and sea air while the aircraft is on the ground near the ocean or on the deck of an aircraft carrier.

B. Environmental Durability of Ceramic and Glass-Ceramic Materials and Composites

While ceramic materials such as silicon nitride and silicon carbide are quite resistant to oxidation due to the formation of a protective silica layer, they are susceptible to hot corrosion due to the dissolution of the silica layer by sodium sulfate[6,7]. Materials such as cordierite (MAS) can also be susceptible to sodium sulfate hot corrosion, but the reaction is much less severe than with silicon carbide or nitride[6]. It was found that the corrosion of cordierite in a burner rig at 1000°C resulted in the formation of sodium aluminosilicate and magnesium silicate, with resulting microcrack formation. It was postulated that the microcracking was caused by either grain boundary glass devitrification due to sodium impurities forming a new phase with a larger volume, or by sodium sulfate penetration into the cordierite causing cracking on cooling.

CVI SiC matrix composites reinforced with Nicalon SiC fibers were investigated in oxidative and corrosive environments by James, et al[8]. It was found that the interface, which consisted of a pre-deposited carbon layer, oxidized at 1000°C in very short times with resultant degradation in composite properties. Combustion environments hastened the degradation and embrittlement of the composites. It was found that exposure to water vapor and/or sulfur accelerated the oxidation process, while exposure to sodium weakened the composites due to a sodium containing glass being formed that tended to dissolve the composite, both fibers and matrix.

The corrosion of CAS glass-ceramic matrix/Nicalon fiber composites by sodium sulfate has been studied by Wang, et al[9,10]. It was found that exposure at 900°C caused severe cracking of the CAS matrix, which, in turn, allowed penetration of the oxidizing atmosphere into the composite interior with resultant composite strength degradation and embrittlement. Similar work by the same authors[11] found that LAS matrix composites were not attacked severely by a thin layer of sodium sulfate at 900°C, but that complete immersion of the samples in molten sodium sulfate resulted in severe attack.

Another type of corrosion reaction to be concerned about is that of reactions due to ceramic to metal contact. For ceramic composites to be utilized in gas turbine engines, they will undoubtedly have to be attached to or come in contact with high temperature nickel based superalloys. In some cases, the ceramic composite/metal interface temperature may be high enough to cause chemical reaction between the composite and metal. Such reactions could change the chemistry of the ceramic composite and could also result in dissolution of the protective oxide scale which is present on nickel-based superalloys.

Reactions at glass-ceramic matrix composite/metal interfaces have been observed previously at UTRC. Studies performed under a NASC program[12] showed that LAS matrix/Nicalon fiber composites reacted with both MAR-M-200 and Hastelloy X superalloys above ~800°C in air. The alumina forming MAR-M-200 alloy reacted very severely with the composites above 900°C, with an unprotective nickel oxide scale forming on the superalloy instead of the protective alumina scale. The chromia forming Hastelloy X reacted much less severely. It was proposed that the lithia present in the LAS matrix was reacting with the protective scales, especially alumina, forming volatile reaction products that resulted in an unprotective nickel oxide scale being formed on the superalloy. BMAS matrix composites may be much more stable in this regard than the previously tested LAS matrix composites. The effect of sulfidation on glass-ceramic/metal reactions has not been studied, however it may be of concern since sulfidation attacks the protective oxide scales formed on superalloys.

As mentioned previously, moisture is also a concern for ceramic materials operating in a gas turbine environment. With respect to glass-ceramic matrix composites, moisture has long been known to have a detrimental effect on the strength of glasses due to stress corrosion effects. Whether this effect manifests itself in glass-ceramic matrix composites is not known, although water/furnace cycling tests to 800°C at P&W on boron doped LAS matrix/Nicalon fiber composites (UTRC-200) have resulted in severe degradation in mechanical properties.

III. TECHNICAL DISCUSSION

A. Materials and Composite Fabrication

During the past year, the CMC material investigated under this program consisted of a barium-magnesium aluminosilicate (BMAS) glass-ceramic matrix, reinforced with Nicalon SiC fibers that had a CVD interfacial coating that consisted of ~300nm of BN overcoated with ~200nm of SiC. The BMAS matrix, when crystallized or "ceramed" at 1200°C for 24 hrs in Ar, converts to the barium osumilite ($BaMg_2Al_6Si_9O_{30}$) phase. The SiC/BN interfacial coating(s) were applied to the Nicalon fibers in an atmospheric pressure continuous CVD reactor by 3M, St. Paul, MN. In this composite system, as mentioned previously, the BN layer acts as the weak, crack deflecting interfacial phase, while the SiC layer acts as a diffusion barrier that prevents BN diffusion into the matrix and matrix element diffusion into the BN during composite fabrication[1]. The interfacial microstructure of this composite system can be seen in the TEM thin foil micrograph shown in Fig. 1. Note the elongated nature of the barium osumilite grains and the small amount of residual glassy phase present at the barium osumilite grain/SiC coating junction.

Three different BMAS matrix/SiC/BN/Nicalon fiber composites were fabricated for use on this program during the past year. All of these composites were fabricated under the usual hot-pressing procedure at a maximum temperature of 1430°C, for 5 min, in Argon, followed by a ceraming step at 1200°C, 24 hrs, in Argon. Each composite consisted of twelve plies oriented in a balanced 0/90° layup. The volume fraction of fibers ranged from 43-48%. Composite #154-93 was pressed in a 6" x 9" (15.2 x 22.8 cm) die, while composites #135-92 and #211-93 were 4" x 4" (10.2 x 10.2 cm) in size. The larger composite (#154-93) was utilized for moisture and sodium sulfate corrosion testing, while the other two composites were utilized for burner rig testing, with and without synthetic sea salt added to the flame.

B. BMAS Glass-Ceramic Matrix Composite Characterization

BMAS matrix/SiC/BN coated Nicalon fiber composite #154-93 was machined into a number of flexural test samples of dimensions 3" long x 0.2" wide x 0.1" thick (7.6 x 0.51 x 0.25 cm), and tensile test samples of dimensions 4" long x 0.5" wide (10.2 x 1.27 cm), with a dog-boned gauge section of dimensions 1" long x 0.2" wide (2.54 x 0.51 cm). The flexural tests were performed in air in 3-pt loading with a span of 2.5" (6.35 cm) and a cross-head speed of 0.05"/min (0.13 cm/min), at temperatures of 22°, 1100°, 1200°, and 1300°C. The tensile tests were performed in air at a loading rate of 0.05 cm/min, at temperatures of 22° and 1100°C. Stepped tensile stress-

rupture tests were also performed at 1100°C. Composite #135-92 was also machined into flexural and tensile test samples after being subjected to burner rig testing. Composite #211-93, which was subjected to burner rig testing with synthetic sea salt added to the flame, was only tested in RT flex before and after burner rig testing, due to the severe corrosive attack that occurred during the sea salt burner rig testing.

1. Moisture Exposure Testing

As mentioned in the Background section, one of the concerns in utilizing CMC's in gas turbine engine applications is that of moisture or water attack on either the matrix or the fiber/matrix interfacial region. While dense matrix CMC's, such as the glass-ceramic matrix composites being studied this past year, are not as likely to experience ingress of water or moisture into the matrix that porous matrix CMC's would, such as the polymer pyrolysis (PIP) or CVI matrix CMC's, they still could be moisture sensitive, especially the BN containing fiber/matrix interfacial region.

It was thus decided to subject BMAS matrix/SiC/BN coated Nicalon fiber composite #154-93 to a series of humidity and moisture tests. One of these tests consisted of a cyclic humidity test where flexural test samples were cycled five times between a humidity chamber at 60°C, 95% RH, into a furnace at 1100°C that contained flowing oxygen. Each cycle consisted of 20 hrs in the humidity chamber and then 20 hrs in the 1100°C furnace. Another test consisted of cycling test samples between a water bath at 80°C and an air furnace at 1100°C for a total of 100 cycles. Each cycle consisted of 20 min in the furnace and 5 min in the water bath. This test was not a thermal shock test, since the samples took about 2.5 min to exit the furnace into the water bath, and vice versa. The final moisture test consisted of pre-stressing the flexural test samples to 35 ksi (240 MPa) in 3-pt flex, which is above the usual matrix microcrack proportional limit stress of ~26 ksi (180 MPa) and thus simulates a damaged composite component, and then subjecting them to the above water/1100°C furnace cyclic test for 100 cycles. All of these tests were meant to simulate a situation where a gas turbine engine component, such as an augmentor seal or nozzle flap, would be subjected to a humid or rain environment, and then be quickly heated to maximum temperature as would be experienced in a scramble take-off situation.

After the humidity and moisture exposures, the test samples were subjected to 3-pt flexural testing at RT, 1100°, 1200°, and 1300°C in air, and compared to baseline values for as-ceramed composite material. The results of these tests are shown in Table I. As can be seen from Table I, none of these humidity or moisture/furnace environmental exposure tests had any effect on the ultimate flexural strength, elastic modulus, or strain-to-failure of the BMAS matrix/SiC/BN coated Nicalon fiber composite material. Even those samples that were pre-stressed beyond their matrix

microcrack limit, thus exposing the fiber/coating/matrix interfacial region to the moisture and furnace atmosphere, did not show any degradation in flexural properties as a result of this exposure. Previous water/furnace cyclic testing at P&W conducted on LAS glass-ceramic matrix/Nicalon fiber composites with *in-situ* formed carbon fiber/matrix interfacial regions, as well as other types of CMC's, such as CVI SiC/SiC, showed a significant amount of composite strength degradation after these environmental exposures.

It appears that the interfacial coating system utilized in the present composite system, CVD SiC over BN, is quite resistant to moisture and humidity, even when it is exposed to these environments due to microcracks in the normally dense BMAS glass-ceramic matrix. A sample of 3M BN coated Nicalon fiber (no SiC overcoat) was subjected to a 14 day exposure at 95% RH at 140°F (60°C). The resultant average RT UTS of the exposed fibers was 398 ksi (2.74 GPa), which is stronger than most as-coated fibers. A scanning Auger depth profile analysis of a BN coated Nicalon fiber that had been exposed to 100% RH at 120°F for 72 hrs showed no change in the composition or morphology of the BN coating. This is contrary to the results of Matsuda[13], who found that BN deposited from boron trichloride plus ammonia at temperatures below ~1400°C was very unstable in the presence of moisture, with the formation of ammonium borate hydrates occurring.

The different results found for the 3M BN coated Nicalon fibers are possibly due to the very low oxygen content of the 3M BN (<4%), and the fact that the 3M BN contains ~15%C, and is most likely deposited from a precursor other than boron trichloride plus ammonia. The exact precursor utilized by 3M to deposit the BN fiber coatings is not known, since it is considered proprietary by 3M. One other difference is that Matsuda utilized powdered BN samples for his studies, with their resultant very high surface areas compared to the coated fibers. In any case, environmental degradation of the BMAS matrix/SiC over BN coated Nicalon fiber composite system caused by humidity or moisture exposure does not appear to be a problem, at least under the conditions utilized under this program.

2. Oxidation and Corrosion (Na_2SO_4) Furnace Exposure Testing

a. Flexural Testing

Flexural samples of BMAS matrix/SiC over BN coated Nicalon fiber composite #154-93 were exposed to a flowing oxygen environment for 100 hrs at temperatures of 900°, 1000°, and 1100°C, both in the as-cerамed condition and after being coated with ~5 mg/cm^2 of sodium sulfate. The samples were weighed after one, ten, and 100 hrs of exposure. After exposure, the samples were subjected to flexural testing at RT, 1100°, 1200°, and, in some cases, 1300°C, with

the results being compared to baseline flexural properties of as-ceramed samples. Analyses conducted on exposed samples consisted of SEM, electron microprobe, scanning Auger, X-ray diffraction, and ESCA examination of composite surfaces, electron microprobe and TEM replica analyses of polished composite cross-sections, and TEM thin foil analysis of selected regions of the composite.

The results of flexural testing of the oxidized and sodium sulfate coated composite samples, compared to as-ceramed samples, are presented in Table II. Some of the elevated temperature tests were limited to ultimate flexural strength determinations only, due to problems with the extensometry used to determine flexural modulus and strain-to-failure. From the results presented in Table II, it can be seen that the flowing oxygen exposures at 900°, 1000°, and 1100°C for 100 hrs, on samples that were not coated with sodium sulfate, did not decrease the flexural strength, elastic modulus, or strain-to-failure of the BMAS matrix/SiC over BN coated Nicalon fiber composites. For the samples coated with sodium sulfate, the flexural strength values did appear to be decreased somewhat (15-30%) for all exposure temperatures. No significant decrease was noted for the composite elastic modulus or strain-to-failure, however.

The weight changes recorded for the exposed composite samples are presented in Table III. It can be seen that the samples not coated with sodium sulfate showed essentially no measurable change in weight after the oxidation exposures. Those coated with ~30mg of sodium sulfate lost weight after one hour of exposure, with no significant weight changes occurring between one hour of exposure and 100 hrs. This loss in weight is undoubtedly due to the evolution of SO_3 during the exposure test. All samples ended the exposure testing with weight gains of between 10 and 17 mg. It is obvious that reactions are occurring between the sodium sulfate and the BMAS matrix composite at all temperatures from 900°-1100°C, even though under the conditions utilized, Jacobson's analysis for the boundaries of sodium sulfate hot corrosion of silica layers under equilibrium conditions[7], predict that above the dew point of sodium sulfate (~954°C) it will not stay in a condensed form, and thus corrosion will not occur. In the present case, however, equilibrium conditions may not exist, and the BMAS matrix is a much more complex system than pure silica.

Figures 2, 3, and 4 show the flexural samples that were coated with sodium sulfate and exposed in gently flowing oxygen for 100 hrs at 900°, 1000°, and 1100°C, respectively. As can be seen in these figures, a glassy, bubbly, scale has formed on the composite surfaces, with the amount of visible bubbling generally increasing somewhat with temperature. In comparison to the composite samples that were oxidized with no sodium sulfate coating, as shown in Fig. 5, the coated samples definitely exhibited surfaces that were more reacted.

b. Microstructural and Chemical Analyses

A variety of analyses were conducted on the composite samples that were coated with sodium sulfate and then subjected to the high temperature oxidation exposures, in order to identify the surface and sub-surface reactions that had occurred and the reaction products formed.

(1). Surface Analyses

Figure 6 shows an electron microprobe analysis of the surface of the composite oxidized at 1100°C for 100 hrs with a sodium sulfate coating, while Fig. 7 shows the same composite surface in a region that was not coated with sodium sulfate. While both surfaces appear somewhat rough, with both obviously crystalline and rather amorphous appearing features, the amount of glazing and cracking and the size of the features is greater for the composite that was coated with sodium sulfate. Area one in Fig. 6 appears to consist of a magnesium silicate, with very little sodium and aluminum and no barium, while area 4 in Fig. 6 appears to consist of a barium aluminosilicate, with some sodium but no magnesium. In Fig. 7, the surface appears to consist of a barium-magnesium aluminosilicate phase (barium osumilite) plus a region rich in magnesium. In Fig. 8, which shows the sodium sulfate coated surface at higher magnification, at least three distinct phases can be seen: Area 1, which appears to consist of a silicate glass with some aluminum; Area 5, which appears to consist of magnesium silicate crystals; and Area 6, which appears to be crystalline barium aluminosilicate, with a small amount of sodium. A small amount of carbon is also present in all of the regions of the oxidized composite, whether coated with sodium sulfate or not.

In order to analyze just the very surface of the oxidized composite, a scanning Auger surface analysis was conducted on a sample that was coated with sodium sulfate and then oxidized at 1000°C for 100 hrs. Figure 9 shows a scanning Auger elemental map for Ba, Al, and Mg of a region with a significant number of needle-like crystals on the composite surface. From this map, it can be seen that the needle-like phase is high in Mg, with no Ba or Al, while other, more blocky crystals are high in Ba and Al, with no Mg. From the scanning Auger chemical analysis shown in Fig. 10, the needle-like phase is confirmed to be a magnesium silicate, the blocky crystals a barium aluminosilicate, and the rest of the surface a barium-magnesium aluminosilicate. Interestingly, no sodium was detected by the scanning Auger analysis of the composite surface.

From X-ray diffraction analysis of the oxidized surface of a sodium sulfate coated composite sample, as shown in Fig. 11 along with the X-ray pattern of an as-ceramed composite, it is obvious that the magnesium silicate and barium aluminosilicate crystals seen in the electron microprobe

and scanning Auger analyses, consist of enstatite ($MgSiO_3$) and celsian ($BaAl_2Si_2O_8$), while the BMAS phase is the normal barium osumilite matrix. While the scanning Auger and X-ray diffraction analyses did not detect any sodium containing phases, the electron microprobe analyses (Figs. 6-8) did detect very slight amounts of sodium in some regions of the oxidized composite surface. The presence of sodium was confirmed by the ESCA, or XPS (X-ray photoelectron spectroscopy), analysis of a composite surface as shown in Fig. 12. In this analysis, in which a rather large area (1mm) of the composite surface is analyzed, a significant amount of sodium (~4.5 at %) was detected. The reason that sodium was not detected from the scanning Auger analysis is that sodium is known to migrate away from the concentrated electron beam in the scanning Auger analysis of amorphous materials.

A possible reaction sequence is that the Nicalon fibers that are exposed to the surface oxygen may be oxidized to silica, with the sodium sulfate then reacting with the crystalline barium osumilite matrix and the silica to form crystalline celsian and enstatite, plus a silica rich sodium aluminosilicate glass and sulfur trioxide gas:

$$BaMg_2Al_6Si_9O_{30} + 2Na_2SO_4 + 7SiO_2 \Rightarrow BaAl_2Si_2O_8 + 2MgSiO_3 + 2Na_2Al_2Si_6O_{16} + 2SO_3 \quad (2)$$

A similar scenario was postulated as the mechanism for the sodium sulfate corrosion of cordierite (MAS) glass-ceramic composites[3]. The sodium containing glassy phase then may continue to react with the SiC/BN coated Nicalon fibers.

(2). Sub-Surface Analyses

Polished cross-sections of BMAS matrix/SiC/BN coated Nicalon fiber composite #154-93 flexural samples with sodium sulfate coatings that had been exposed to flowing oxygen at 1100°C for 100 hrs were subjected to electron microprobe and TEM replica analyses. In addition, TEM thin foil analyses were conducted on the fiber/coating(s)/matrix interfacial regions of the composites. Figure 13 shows electron microprobe elemental scans taken from a polished corner section of an exposed flexural sample. It can be seen that the surface of the sample has become quite rough, with an obviously reacted region extending 100 to 300 microns into the composite. A significant amount of porosity can be seen in the reacted region, along with magnesium rich phases coupled with a considerable amount of sodium diffusion into the composite. A higher magnification elemental scan is shown in Fig. 14, with severely reacted Nicalon fibers in a glassy phase that obviously contains crystalline phases that are either rich in Mg or Ba. Another micrograph of the region detailed in Figs. 13 and 14 is shown in Fig. 15, and appears to indicate that the corrosion of the 0/90° layup composite is more severe for the 90° layers that are exposed to the environment than for the 0° layers.

TEM replica and thin foil analyses were also performed on the region of composite #154-93 that was shown in Figs. 13-15. The TEM replica characterization shown in Figs. 16 and 17 indicates that the attack of the coated Nicalon fibers is very localized to the region near the composite surface that consists of the sodium containing glassy phase, and appears to selectively initiate in the SiC/BN coating. TEM thin foil analysis verifies that the BN layer within the SiC/BN coating is being attacked first by the sodium containing glassy phase. Figure 18 shows two SiC/BN coated Nicalon fibers separated by a glassy matrix phase at the very edge of the reacted region of the composite. The SiC/BN layer is intact on the lower fiber in Fig. 18, while on the upper fiber, the BN layer is very spotty and appears to have been partially dissolved by a glassy phase. The upper fiber in Fig. 18 also appears to have a somewhat enlarged grain size, compared to the lower fiber.

Figure 19 shows a TEM thin foil micrograph of a region closer to the composite surface where the Nicalon fibers have been severely attacked. The Nicalon fiber appears to be separated from the glassy matrix by two regions: (1) a somewhat discontinuous light colored zone that contains primarily Si and O, with minor amounts of other matrix elements such as Mg, Al, and Ba, but with significant amounts of Na and S; and (2) a continuous layer next to the fiber surface that is primarily Si and O, with minor Na. Figure 20 shows selected area electron diffraction patterns of the glassy matrix (1), the Nicalon fiber (3), and the light colored reaction product (2) that contained the Na and S. This reaction product is crystalline in nature and is currently in the process of being identified.

c. Tensile Testing

Tensile tests were performed on BMAS matrix/SiC/BN coated Nicalon fiber composite #154-93 at RT, and at 1100°C in air with and without sodium sulfate coatings on the gauge section of the tensile samples. In addition, stepped tensile stress-rupture testing was performed at 1100°C, with and without sodium sulfate coatings. The tensile stress-rupture testing was initiated at a stress of 12 ksi (83 MPa), which is approximately equal to the proportional limit, or matrix microcrack, stress in tension at 1100°C. The stress was held for ~50 hrs, then increased in 2 ksi (13.8 MPa) increments, with a hold of ~50 hrs at each stress level, until failure. The results of these tests are presented in Table IV.

From Table IV, it can be seen that the tensile strength of composite #154-93 is ~ 46 ksi (317 MPa) at RT, increasing slightly to ~50 ksi (344 MPa) at 1100°C. The strain-to-failure also increased somewhat from RT to 1100°C, while the elastic modulus decreased. This is due to the slight softening of the residual glassy phase present in the matrix between the barium osumilite grains. The results for composite #154-93 are comparable to previously obtained values for other

composites in the BMAS matrix/SiC/BN coated Nicalon fiber composite system[1,2]. With ~4mg/cc sodium sulfate coated on the gauge section of the tensile sample, the short time 1100°C tensile properties of the composite are essentially unaffected.

The stepped tensile stress-rupture properties of the uncoated composite sample at 1100°C are in the lower end of the range of previously tested 0/90° ply lay-up BMAS matrix/SiC/BN coated Nicalon fiber composites. These composites usually fail at stress levels of 28-34 ksi (193-234 MPa), and total times of 500-900 hrs. With sodium sulfate coated on the gauge section, however, the tensile stress-rupture failure stress dropped to 22 ksi (152 MPa) after an exposure time under stress of only 266 hrs. While the fracture surface of this sample appeared quite fibrous, there was a significant amount of surface bubbling and glazing, similar to the furnace exposed composite sample that was shown in Fig. 4. Further analysis of the sodium sulfate coated tensile and tensile stress rupture samples is currently in progress.

3. Burner Rig Testing

Burner rig thermal fatigue testing of BMAS matrix/SiC/BN coated Nicalon fiber composite panels was conducted at Pratt & Whitney, E. Hartford, CT. The impingement burner rig used in this program has a 2" (5.1 cm) diameter nozzle, burns standard jet engine "jet A" fuel, and has a hot gas velocity of 0.7 Mach. The high gas velocity and the flame impingement result in vibration and erosion actions that simulate the actual gas turbine engine environment. A schematic of the burner rig utilized is shown in Fig. 21, with the provision for continuously aspirating a synthetic sea salt solution into the flame during the test. Figure 22 shows the burner rig in operation with an LAS matrix composite panel in the test fixture. Burner rig thermal fatigue testing of a variety of LAS matrix composites was conducted previously under a NADC program[14].

The burner rig test cycle utilized under the current program consisted of a 1100°C maximum temperature on the front face of the panel, with the panel being cycled in and out of the flame for 6000 cycles. The test cycle consisted of 50 seconds of burner exposure and 10 seconds of forced air cool when the specimen is away from the burner. During the forced air cool, the temperature of the front face of the panel decreased to less than 600°C. The BMAS matrix composite panels were held in place with slotted posts of PWA 1480 nickel based superalloy.

a. Burner Rig Testing Without Sea Salt Added to the Flame

Figure 23 shows the visual appearance of the hot side of BMAS matrix/SiC/BN coated Nicalon fiber composite panel #135-92 after the 1100°C, 6000 cycle, burner rig test with no injected sea

salt, and the ultrasonic NDE analyses of this panel both before and after the burner rig test. A detailed description of the ultrasonic NDE techniques and equipment utilized at UTRC to conduct these tests has been given in Ref. 15, and will not be repeated here. The NDE analyses were run at a frequency of 25 MHz with an attenuation range of 0 to 126 dB/cm. The frequency and attenuation scale was chosen so that some structure of the panels could be detected, such as the 0/90° plies and surface imperfections transferred to the composite surface from scratches or nicks in the graphite dies used to hot-press the panels.

From Fig. 23, it can be seen that the composite hot surface shows very little evidence of the burner rig test, other than a slight discoloration in the center (hot) region, and some indications on the sides of where the panel was held by the superalloy slotted posts. No visible interaction occurred between the BMAS matrix composite and the nickel based superalloy posts, unlike previous studies[15] where obvious reactions were seen along the edges of LAS matrix composite panels subjected to identical burner rig testing at a maximum temperature of 985°C. The ultrasonic NDE analyses shown in Fig. 23 before and after burner rig testing are very similar, with little change in the ultrasonic wave attenuation. The one attenuated spot that can be seen on the left side of both NDE analyses is a surface imperfection caused by a gouge in the graphite spacer utilized during composite fabrication.

Figure 24 shows an electron microprobe elemental map of a polished cross-section of the hot face of composite #135-92 after the 1100°C, 6000 cycle, burner rig test. No differences can be seen in the elemental distribution in the matrix from the surface to interior, nor can any obvious attack of the Nicalon fibers be seen near the hot face of the composite.

After the burner rig testing, composite #135-92 was machined into flexural and tensile samples, and subjected to flexural tests (hot side in tension) at RT, 1100°, and 1200°C, tensile tests at 1100° and 1200°C, and a stepped tensile stress-rupture test at 1100°C. The results of these tests are shown in Table V. As can be seen from the data in this table, the flexural and tensile properties of this composite were as high, or higher, than that measured on the as-ceramed composite #154-93, as reported in Tables I and IV. The 1100°C stepped tensile stress-rupture test resulted in a final fracture stress of 32 ksi (220 MPa), after 730 hrs in air under gradually increasing stress levels. This fracture stress is ~70% of the ultimate short time tensile strength at 1100°C. It can thus be concluded that burner rig exposure at an 1100°C maximum temperature for 6000 cycles in a Mach 0.7 burner flame does not degrade the properties or significantly affect the microstructure of the BMAS matrix/SiC/BN coated Nicalon fiber composite system.

b. Burner Rig Testing With Sea Salt Added to the Flame

An 1100°C, 6000 cycle, burner rig test was conducted on BMAS matrix/SiC/BN coated Nicalon fiber composite panel #211-93, with an aqueous solution of synthetic sea salt continuously aspirated into the flame at a concentration level of ~5 ppm. The composition of the synthetic sea salt was ~27.35 wt% Na^+, 6.8% Mg^{++}, 0.8% Ca^{++}, 6.0% $SO_4^=$, and 59.05% Cl^-. The test was interrupted at ~3000 cycles to photograph the panel hot side surface.

The front (hot) surface of composite #211-93 after 3000 cycles at 1100°C in the burner rig with 5 ppm sea salt aspirated into the flame is shown in Fig. 25. As can be seen, a significant amount of corrosion occurred during the 3000 cycle (50 hr) burner rig exposure. The surface had the appearance of a glassy flow radiating out from the center of the panel where the burner flame was concentrated. The nickel based superalloy posts holding the panel in place were also severely corroded, as shown in the higher magnification photo in Fig. 26.

After completing the 6000 cycle (100 hr) burner rig test, composite #211-93 exhibited additional distress, as shown in Fig. 27. The surface of the composite panel was severely eroded, and the amount of glassy droplets concentrated around the edge of the panel had increased during the additional 3000 cycles. While not shown in Fig. 27, the metal superalloy posts were almost corroded away to the point of not being able to hold the composite panel in place.

After the completion of this test, the composite panel #211-93 was machined into flexural samples. The side of one of these flexural samples machined from the center region of the panel is shown in a photo montage from end to end in Fig. 28. It can be seen that in the center region of the panel, approximately half of the panel thickness has been corroded away. The large glassy droplets can be seen to be concentrated near the edges of the panel surface. No corrosion occurred on the back (cool) side of the panel, with the only effect being near the edges where glassy droplets have migrated around the panel edge from the front side.

The only mechanical property tests conducted on composite panel #211-93 were two RT 3-pt flexural tests, one from the edge of the panel prior to the sea salt burner rig exposure, and one after exposure. The test after exposure was conducted on the sample shown in Fig. 28, with the back, or smooth, side in tension, and the reduced thickness measured as close as possible from Fig. 28. Taking this reduced thickness into account, the strength of the remaining composite material after the sea salt burner rig exposure [66 ksi (454 MPa)] was approximately the same as that prior to the exposure [71 ksi (490 MPa)]. Thus, the composite material that was not totally corroded was not degraded in strength by the sea salt burner rig exposure.

One of the flexural samples was subjected to wet chemical analysis, including a water leach test to detect water soluble salts. Only a small amount of Na and SO_4^{-2} water soluble salt was detected, however a significant amount of both acid soluble (glassy) and acid insoluble (crystalline) impurities of Na and Ca were found, as well as minor amounts of Fe, Co, and Ni. The latter elements are undoubtedly a result of the corrosion of the nickel based superalloy holders or erosion of the burner duct during the test, with subsequent deposition on the composite panel.

To date, the only microstructural analysis conducted on composite panel #211-93 after the sea salt burner rig test was an electron microprobe elemental scan of the corroded surface area. Near the edge of the panel, as shown in Fig. 29, a very thick glassy layer with large pores or bubbles in it has formed on the panel surface. This layer consists of a silicate glass containing the elements Al, Ba, and Mg from the composite matrix, and Na and Ca (and possibly Mg) from the sea salt. No sulfur was detected in the glassy layer from the electron microprobe analysis. The center of the panel, as shown in Fig. 30, had approximately four of the twelve 0/90° plies totally eroded away, with the next two exhibiting partial reaction and erosion. No distinct glassy layer was evident in the center section of the panel, but a significant amount of Na (and some Ca) was detected in the matrix region where partially dissolved Nicalon fibers, plus porosity, could be seen. Figure 30 appears quite similar to the composite surface region shown in Fig. 13 for composite #154-93, that was coated with sodium sulfate and then exposed at 1100°C for 100 hrs in flowing oxygen.

From the results of the burner rig test conducted with synthetic sea salt being continually aspirated into the flame during the 6000 cycle test, it was apparent that this exposure condition was much too severe to realistically simulate the conditions that might be encountered in a gas turbine engine. The fact that the nickel based superalloy posts were severely corroded during the test, and were not directly in the burner flame, confirms that the test conditions were not indicative of what would occur in actual gas turbine engine operation, since superalloy component corrosion of this magnitude is never experienced in the field. A more realistic test may be a cyclic test where the salt is introduced periodically by coating the burner rig sample with synthetic sea salt, which simulates a gas turbine nozzle component that may encounter direct deposition of salt water and sea air or while the aircraft is on the ground near the ocean or on the deck of an aircraft carrier. A burner rig test of this type is recommended for future environmental testing of CMC's.

IV. CONCLUSIONS AND RECOMMENDATIONS

From the results of the first year's work on this program, certain conclusions and recommendations can be made. From the moisture exposure testing done under this program on BMAS matrix/SiC/BN coated Nicalon fiber composites, utilizing both water and humidity/furnace cycling to 1100°C, with both as-fabricated and pre-stressed composites, no degradation in composite flexural properties were seen. It appears that the interfacial coating system utilized in the present composite system, CVD SiC over BN, is quite resistant to moisture and humidity, even when it is exposed to these environments due to microcracks introduced into the normally dense BMAS glass-ceramic matrix. During the next year, similar tests will be conducted on polymer infiltrated and pyrolyzed (PIP) matrix composites. With their inherent surface connected porosity, these types of CMC's may be moisture sensitive.

From the flowing oxygen exposures performed on the BMAS matrix/SiC/BN coated Nicalon fiber composites at 900°, 1000°, and 1100°C, for times of up to 100 hrs, it was found that no decrease in flexural strength, elastic modulus, or strain-to-failure of these composites occurred as a result of these exposure conditions. No significant changes were found in the composite microstructure as a result of these oxidative exposures. From concurrent work being conducted under an AFOSR program[16], it has been found that oxidation of the coated Nicalon fibers that are very close to the composite surface does occur for longer times at 1100° and 1200°C. However, the effect on composite properties is not significant. This may not be the case for the porous matrix PIP CMC systems, which will be investigated during the next year of the program.

For samples coated with sodium sulfate, and then exposed at temperatures of 900°-1000°C in flowing oxygen, degradation of mechanical properties and reactions in the near-surface region of the composite were found to occur. The flexural strength of the composites at RT, 1100°, and 1200°C decreased from 15-30% for all exposure temperatures. No significant decrease was noted for the composite elastic modulus or strain-to-failure, however. The short-time tensile strength at 1100°C of the composite coated with sodium sulfate did not decrease, however, a sample tested in stepped tensile stress-rupture at 1100°C did show a significant drop in ultimate fracture stress and total time to failure, compared to a sample with no sodium sulfate coating.

The appearance of the surface of the composite samples that were coated with sodium sulfate and then exposed at 900°-1000°C was that of a glassy, bubbly scale, with the amount of visible bubbling generally increasing with temperature. From surface analysis techniques including electron microprobe, scanning Auger, X-ray diffraction, and ESCA, it was found that the

sample surface consisted of a sodium containing glassy phase plus crystals of magnesium silicate (enstatite) and barium aluminosilicate (celsian). Sub-surface analysis of polished composite cross-sections and thin foils verified that the BMAS matrix had reacted to form a sodium containing glassy phase plus enstatite and celsian. The BN fiber coating appeared to be selectively attacked by the sodium containing glassy phase. A possible reaction sequence is that the Nicalon fibers that are exposed to the surface oxygen may be oxidized to silica, with the sodium sulfate then reacting with the crystalline barium osumilite matrix and the silica to form crystalline celsian and enstatite, plus a silica rich sodium aluminosilicate glass and sulfur trioxide gas:

$$BaMg_2Al_6Si_9O_{30} + 2Na_2SO_4 + 7SiO_2 \Rightarrow BaAl_2Si_2O_8 + 2MgSiO_3 + 2Na_2Al_2Si_6O_{16} + 2SO_3$$

The sodium containing glassy phase then appears to further attack the BN coatings and the Nicalon fibers.

It was found that burner rig thermal fatigue testing of a BMAS matrix/SiC/BN coated Nicalon fiber composite panel to a maximum of 1100°C hot-spot temperature for 6000 cycles, without the presence of sodium sulfate, did not degrade the flexural, tensile, or tensile stress-rupture properties of the composite or significantly affect the composite near-surface microstructure. However, with synthetic sea salt being continuously aspirated into the burner flame (~5ppm), the surface of the composite panel and the nickel based superalloy posts that were holding the composite in place became severely corroded, with a significant amount of glassy phase formation and the loss of 4-5 of the twelve plies of coated fibers. Even so, the composite material that was not totally corroded was not degraded in strength or toughness by the sea salt burner rig exposure.

From the results of the burner rig test conducted with synthetic sea salt being continually added to the flame during the 6000 cycle test, it was apparent that this exposure condition was much too severe to realistically simulate the conditions that might be encountered in a gas turbine engine. The fact that the nickel based superalloy posts were severely corroded during the test, and were not directly in the burner flame, confirms that the test conditions were not indicative of what would occur in actual gas turbine engine operation, since superalloy component corrosion of this magnitude is never experienced in the field. A more realistic test may be a cyclic test where the salt is introduced periodically by coating the burner rig sample with synthetic sea salt, which simulates a gas turbine nozzle component that may encounter direct deposition of salt water and sea air or while the aircraft is on the ground near the ocean or on the deck of an aircraft carrier. A burner rig test of this type is recommended for future environmental testing of CMC's, and will be utilized during the next year of the program for both glass-ceramic and PIP matrix composites.

V. ACKNOWLEDGMENTS

The author would like to thank Mr. Bob Brown, Mr. Charles Burila, Dr. Bruce Laube, and Mr. Gerald McCarthy of UTRC for the SEM, electron microprobe, scanning Auger, and TEM analyses, respectively, Ms. Laura Austin and Mr. Stan Kustra of UTRC for the fabrication and mechanical testing of the composites, respectively, Mr. Gary Linsey and Mr. David Murphy of P&W, E. Hartford, for the burner rig and tensile testing of composites, and to Dr. Steve Fishman of ONR for his sponsorship of the program.

REFERENCES

1. Brennan, J., Nutt, S., and Sun, E.: Interfacial Studies of Coated Fiber Reinforced Glass-Ceramic Matrix Composites, Annual Report R93-970150-2 on AFOSR Contract F49620-92-C-0001, November 30, 1993.

2. Sun, E.Y., Nutt, S.R., and Brennan, J.J.: Interfacial Microstructure and Chemistry of SiC/BN Dual-Coated Nicalon-Fiber-Reinforced Glass-Ceramic Matrix Composites, J. Am. Ceram. Soc., 77 [5] 1329-39 (May, 1994).

3. Jarmon, D.C.: Environmental Effects on Reinforced Ceramic Matrix Composites, Seventh Quarterly Report R94-970248-7 on NAWC Contract N62269-92-C-0208, May 15, 1994.

4. Fryxell, et. al.: Theory for Accelerated Turbine Corrosion, Third Conference on Gas Turbine Materials in a Marine Environment, Univ. of Bath, England, Sept. 1976.

5. Bornstein, N.: Proceedings of the 1974 Gas Turbine Materials in Marine Environment Conf., MCIC-75-27, July, 1974.

6. Fox, D.S., Jacobson, N.S., and Smialek, J.L.: Hot Corrosion of Ceramic Engine Materials, NASA TM-101439, DOE/NASA/50111-2, Oct. 1988.

7. Jacobson, N.S.: Corrosion of Silicon-Based Ceramics in Combustion Environments, J. Am. Ceram. Soc., 76 [1] 3-28 (Jan. 1993).

8. James, R.D., Lowden, R.A., and More, K.L.: The Effects of Oxidation and Combustion Environments on the Properties of Nicalon/SiC Composites, Cer. Trans., Advanced Composite Materials, Vol. 19, edited by M. Sacks, A. Cer. S., 1991.

9. Wang, S-W, Kowalik, R.W., and Sands, R.: Strength of Nicalon Fiber Reinforced Glass-Ceramic Matrix Composites After Corrosion With Na_2SO_4 Deposits, Cer. Engr. & Sci. Proc., Vol. 13, No. 9-10, 1992, 760-769.

10. Wang, S-W, Kowalik, R.W., and Sands, R.: High Temperature Behavior of Salt Coated Nicalon Fiber Reinforced Calcium Aluminosilicate Composite, ibid, Vol. 15, No. 4, 1994, 465-474.

11. Wang, S-W, Kowalik, R.W., and Sands, R.: Hot Corrosion of Two Nicalon Fiber-Reinforced Glass-Ceramic Matrix Composites, ibid, Vol. 14, No. 7-8, 1993, 385-398.

12. Brennan, J.J., and Prewo, K.P.: Investigation of Lithium Aluminosilicate (LAS)/SiC Fiber Composites for Naval Gas Turbine Applications, Final Report R83-916232-4 on NASC Contract N00019-82-C-0438, Oct. 30,1983.

13. Matsuda, T.: Stability to Moisture For Chemically Vapour-Deposited Boron Nitride, J. Mat. Sci., 24 (1989) 2353-2358.

14. Brennan, J.J.: The Evaluation and Testing of SiC Fiber Reinforced Glass-Ceramic Matrix Composites, Final Report R91-917812-13 under NADC Contract N62269-87-C-0233, Aug. 6, 1992.

15. Brennan, J.J.: Effect of Thermal and Mechanical Fatigue and Ballistic Impact on Retained Strength of a SiC Fiber Reinforced Glass Matrix Composite, Final Report R86-917276-4 on NADC Contract N62269-85-C-0253, Nov. 30, 1986.

16. Brennan, J., Nutt, S., and Sun, E.: Interfacial Studies of Coated Fiber Reinforced Glass-Ceramic Matrix Composites, Final Report R94-970150-1 on AFOSR Contract F49620-92-C-0001, to be published.

Table I

Flexural Test Results (3-pt) on BMAS Matrix/SiC/BN Coated Nicalon Fiber Composite #154-93 After Various Moisture Exposures (0/90° Fiber Orientation)

Exposure Conditions	Flexural Strength-ksi (MPa) / [E-msi (GPa) / ε_f -%			
	RT	1100°C	1200°C	1300°C
As-ceramed (1200°C, 24hrs, Ar)	74 (512) [18.0 (124)] 0.61%	93 (642) [11.0 (76)] 1.07%	67 (462) [8.5 (59)] 1.06%	45 (308) [6.0 (41)] 1.04%
Cyclic, humidity (95% RH, 60°C) to 1100°C, O_2, 5 cycles (20 hrs/cycle)	76 (524) [18.5 (128)] 0.63%	91 (629) [11.6 (80)] 1.00%	78 (540) [9.5 (66)] 1.05%	48 (330) [7.9 (55)] 0.99%
Cyclic, 80°C water to 1100°C air 20 min furnace, 5 min H_2O (100 cycles)	73 (503) [18.2 (126)] 0.56%	98 (674) [11.6 (80)] 0.98%	73 (503) [9.7 (67)] 1.00%	40 (278) [6.6 (46)] 1.08%
Prestressed to 35 ksi (240 MPa), then cycled from 80°C water to 1100°C air for 100 cycles	70 (483) [17.0 (117)] 0.56%	84 (576) [9.8 (67)] 1.05%	69 (473) [8.7 (60)] 0.99%	-

Table II

Flexural Test Results (3-pt) on BMAS Matrix/SiC/BN Coated Nicalon Fiber Composite #154-93 After Oxidation and Sodium Sulfate Exposures (0/90° Fiber Orientation)

Exposure Conditions	Flexural Strength-ksi (MPa) / [E-msi (GPa) / ε_f -%			
	RT	1100°C	1200°C	1300°C
As-ceramed (1200°C, 24hrs, Ar)	74 (512) [18.0 (124)] 0.61%	93 (642) [11.0 (76)] 1.07%	67 (462) [8.5 (59)] 1.06%	45 (308) [6.0 (41)] 1.04%
900°C, 100 hrs, O_2	66 (457) [20.8 (143)] 0.52%	-	-	-
900°C, 100 hrs, O_2 (Na_2SO_4) (~5 mg/cc Na_2SO_4)	57 (390) [17.5 (121)] 0.48%	47 (321) [9.5 (66)] ?	57 (396) ? ?	-
1000°C, 100 hrs, O_2	73 (505) [19.5 (134)] 0.53%	-	-	-
1000°C, 100 hrs, O_2 (Na_2SO_4) (~5 mg/cc Na_2SO_4)	62 (426) [16.4 (113)] 0.50%	68 (470) [11.8 (81)] ?	60 (415) ? ?	-
1100°C, 100 hrs, O_2	70 (483) [18.6 (128)] 0.65%	73 (505) [10.9 (75)] 0.88%	70 (483) [9.7 (67)] 1.09%	41 (281) [6.8 (47)] 0.86%
1100°C, 100 hrs, O_2 (Na_2SO_4) (~5 mg/cc Na_2SO_4)	52 (356) [17.4 (120)] 0.52%	77 (528) [11.4 (79)] 0.83%	47 (324) [8.5 (59)] 0.99%	-

Table III

Typical Weight Changes As a Result of 100 Hr Flowing Oxygen Exposure for BMAS Matrix/SIC/BN Coated Nicalon Fiber Composite #154-93 Flexural Samples (With and Without Na_2SO_4)

Exposure Temperature	Wt. of Na_2SO_4 Added (mg)	Weight Change After Exposure (mg)			
		1 hr	10 hrs	100 hrs	Total
900°C	none	-1	-1	-1	-1
"	+27	-13	-13	-14	+13
1000°C	none	-2	-2	-2	-2
"	+32	-19	-23	-22	+10
1100°C	none	-1	-1	+1	+1
"	+27	-12	-13	-10	+17

Table IV

Tensile Test Results for BMAS Matrix/SIC/BN Coated Nicalon Fiber Composite #154-93 with and Without Sodium Sulfate (0/90° Fiber Orientation)

Without Sodium Sulfate

Temperature	UTS - ksi(MPa)	PL - ksi(MPa)	E - msi(GPa)	ε_f - %
RT	46 (317)	14.6 (101)	19.2 (132)	0.56
1100°C	50 (317)	12.3 (85)	11.9 (82)	0.76

* 1100°C Stepped Tensile Stress Rupture - 12-28 ksi (83-193 MPa), total 497 hrs

With Sodium Sulfate (~4mg/cc)

Temperature	UTS - ksi(MPa)	PL - ksi(MPa)	E - msi(GPa)	ε_f - %
RT		Not Determined		
1100°C	46.3 (320)	10.7 (74)	10.9 (75)	0.77

* 1100°C Stepped Tensile Stress Rupture - 12-22 ksi (83-142 MPa), total 266 hrs

Table V

Mechanical Properties in Air for BMAS Matrix/SiC/BN Coated Nicalon Fiber Composite #135-92 (0/90°) (After 1100°C, 6000 cycle, Burner Rig Test)

Flexural Properties (Hot Side in Tension)

Temperature	σ - ksi(MPa)	PL - ksi(MPa)	E - msi(GPa)	ε_f - %
RT	100 (690)	26 (180)	20.5 (142)	0.79
1100°C	97 (670)	20 (140)	14.8 (102)	0.86
1200°C	79 (545)	11.5 (79)	11.5 (79)	1.03

Tensile Properties

Temperature	UTS - ksi(MPa)	PL - ksi(MPa)	E - msi(GPa)	ε_f - %
RT	Not Determined			
1100°C	46 (317)	14.6 (101)	11.1 (77)	0.88
1200°C	45 (310)	10.5 (72)	8.0 (55)	0.93

* 1100°C Stepped Tensile Stress Rupture - 10-32 ksi (69-220 MPa), total 730 hrs

Fig. 1 TEM Micrograph of BMAS Matrix/SiC/BN/Nicalon Fiber Composite #119-91

PG232.28

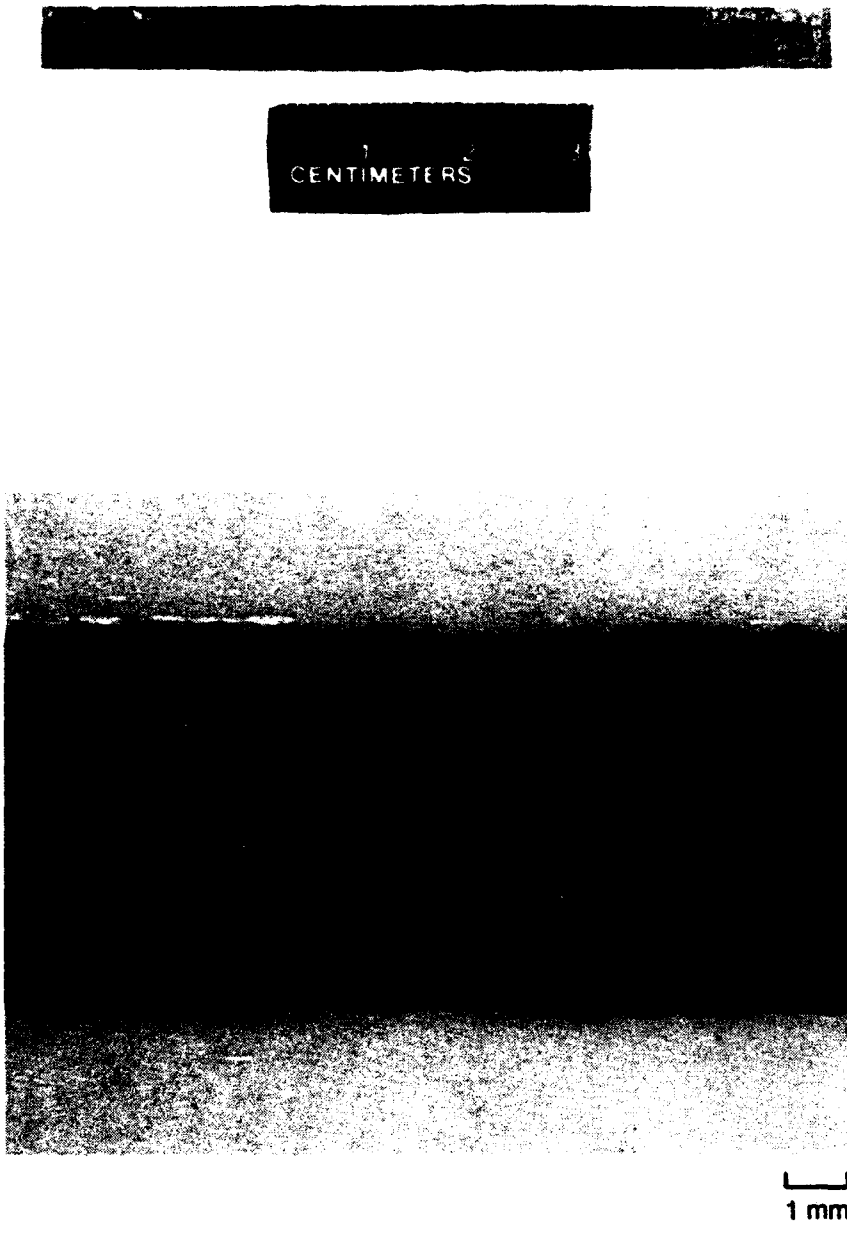

Fig. 2 **Flexural Test Sample of BMAS Matrix/SiC/BN Coated Nicalon Fiber Composite #154-93 (900°C, 100 hrs, O_2, Na_2SO_4)**

PG232.5

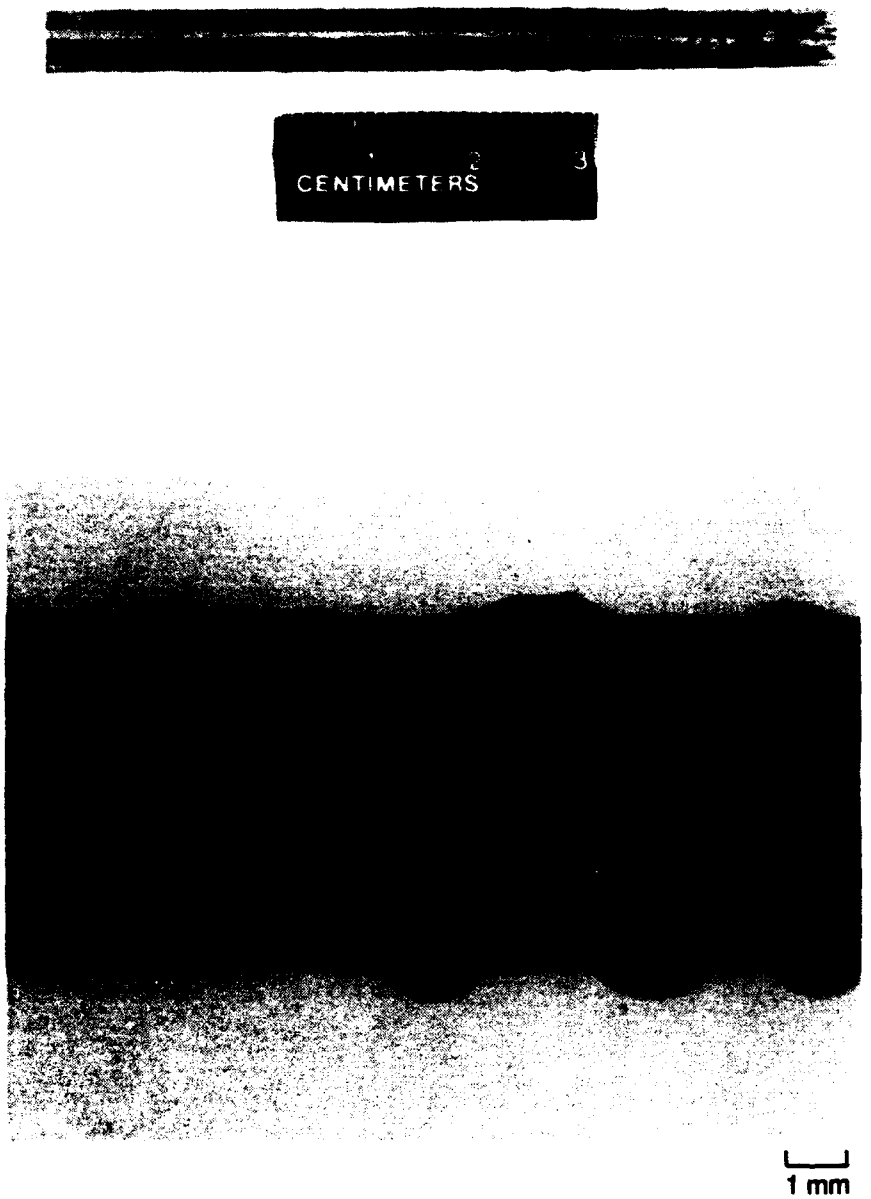

Fig. 3 **Flexural Test Sample of BMAS Matrix/SiC/BN Coated Nicalon Fiber Composite #154-93 (1000°C, 100 hrs, O_2, Na_2SO_4)**

PG232.4

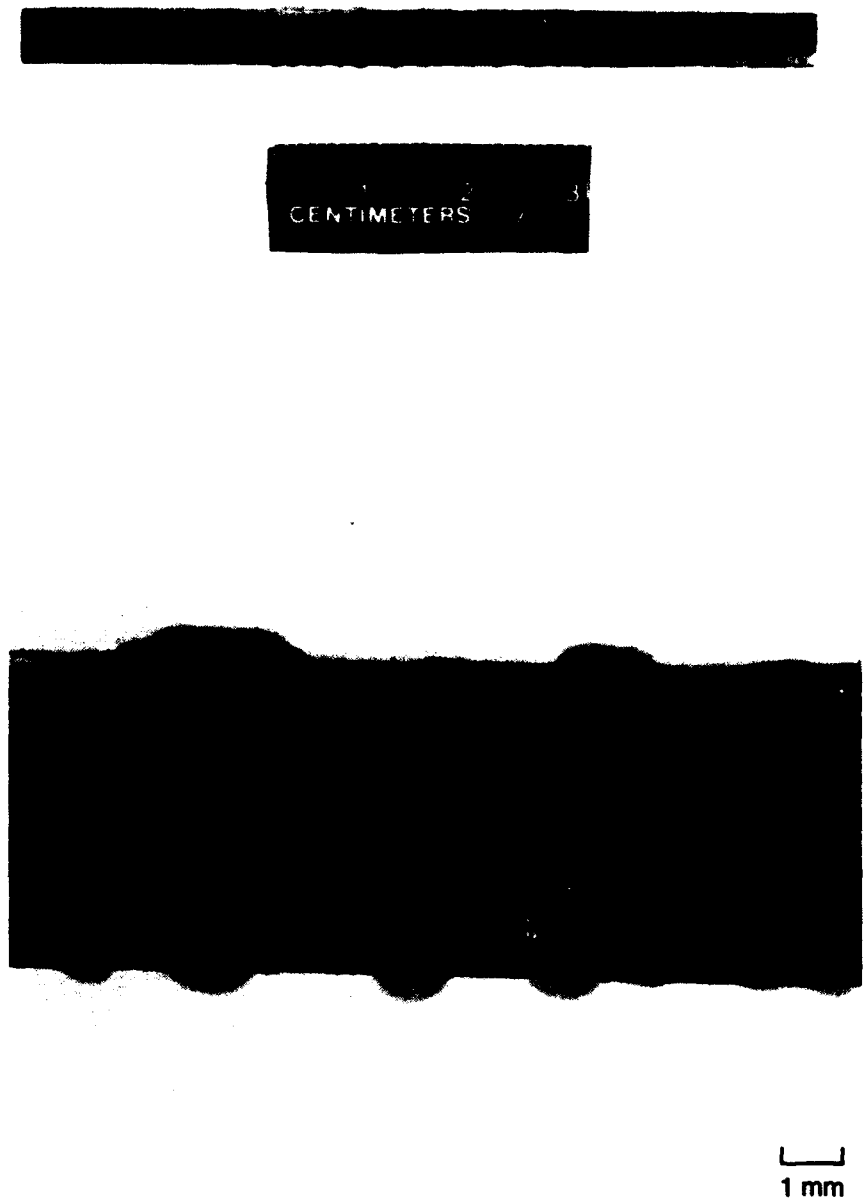

Fig. 4 **Flexural Test Sample of BMAS Matrix/SiC/BN Coated Nicalon Fiber Composite #154-93 (1100°C, 100 hrs, O_2, Na_2SO_4)**

PG232.3

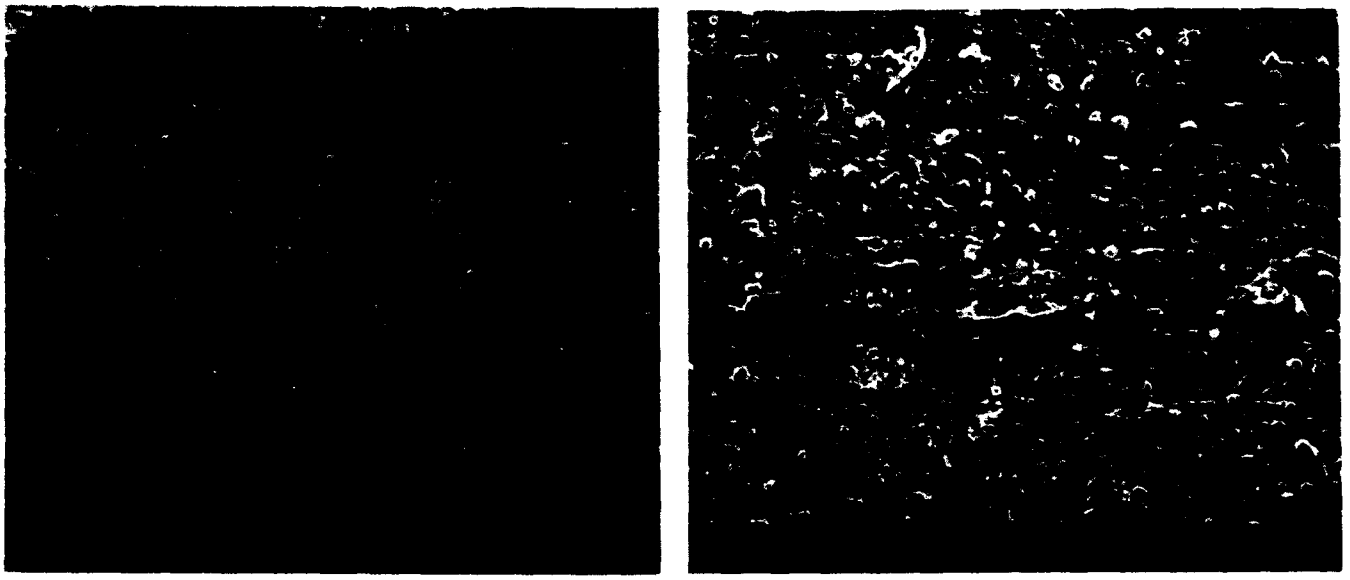

A. Not Coated With Na_2SO_4

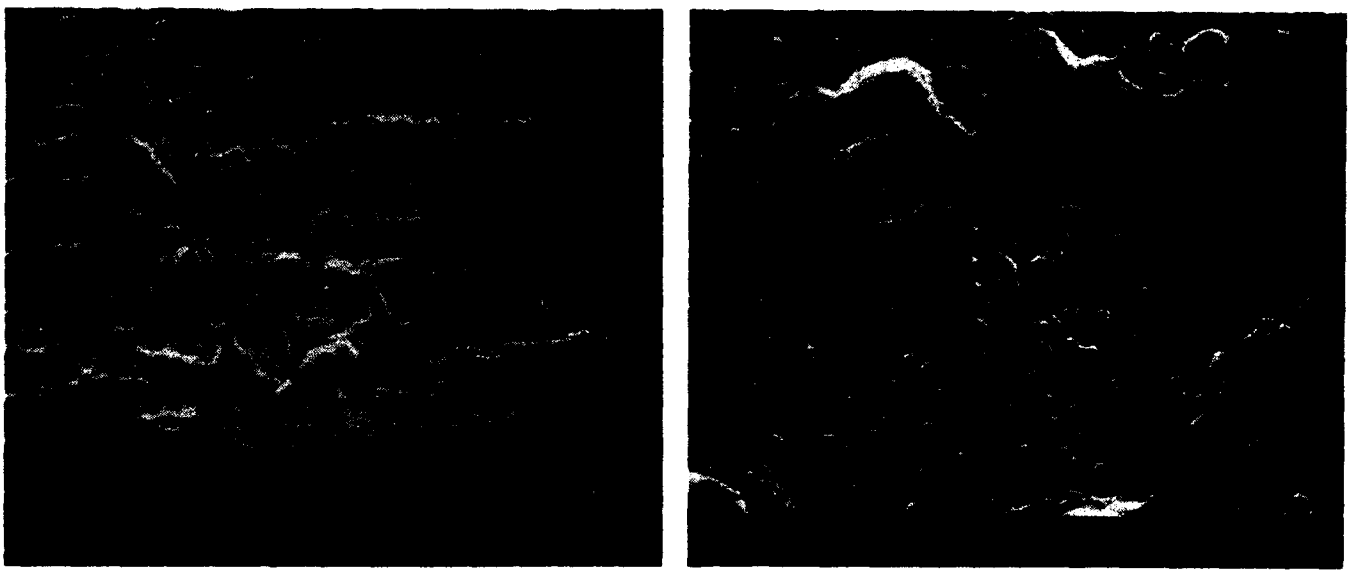

B. Coated With Na_2SO_4

Fig. 5 Surface of BMAS Matrix/SiC/BN Coated Nicalon Fiber Composite #154-93 (1100°C, 100 hrs, O_2)

PG232.7

A. SEM

B. BEI

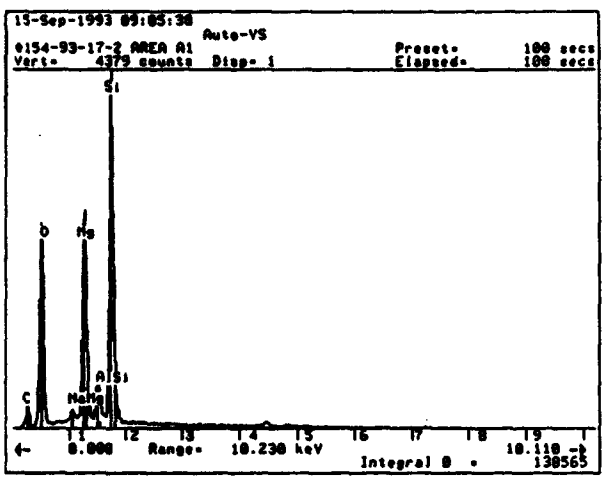

Area 1

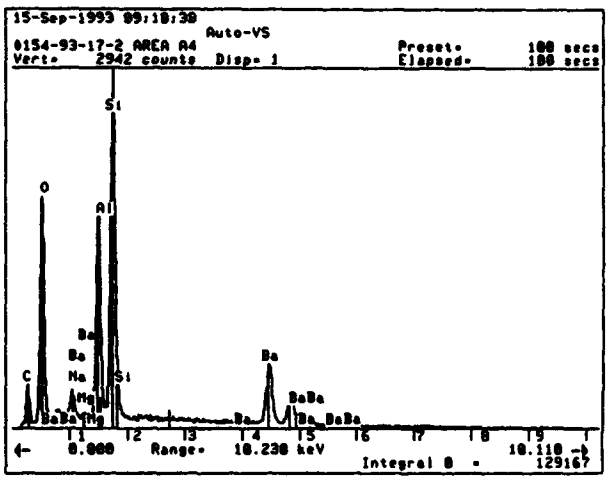

Area 4

Fig. 6 Electron Microprobe Analysis of the Surface of BMAS Matrix/SiC/BN Coated Nicalon Fiber Composite #154-93 (1100°C, 100 hrs, O_2, Na_2SO_4)

PG232.8

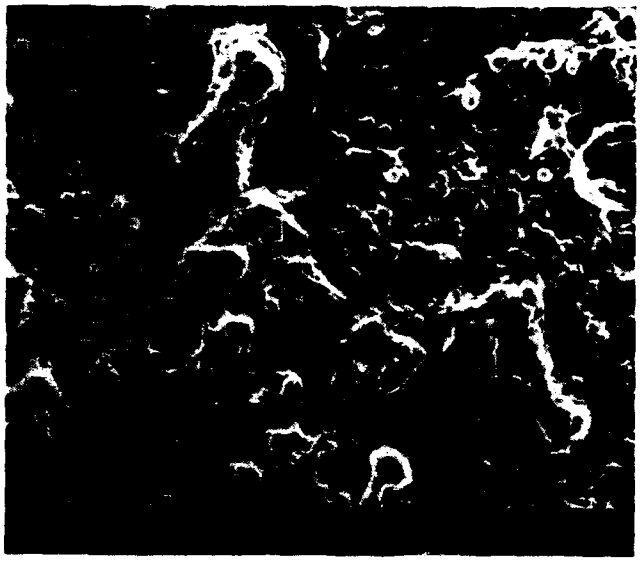

A. SEM

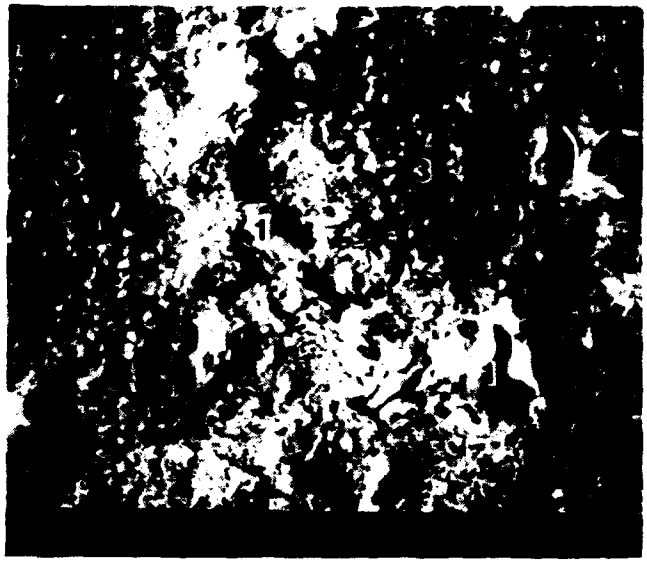

B. BEI

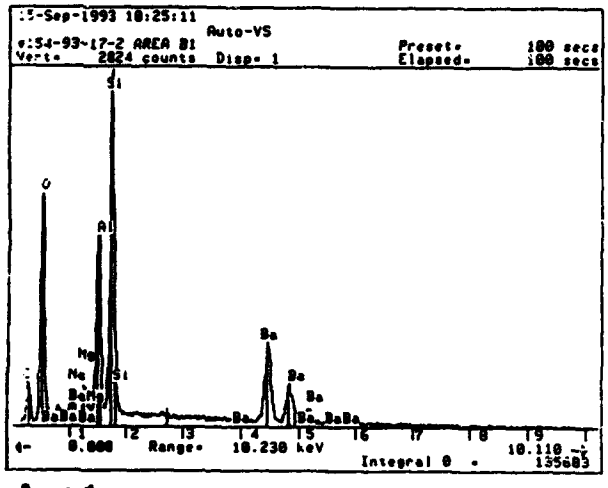

Area 1

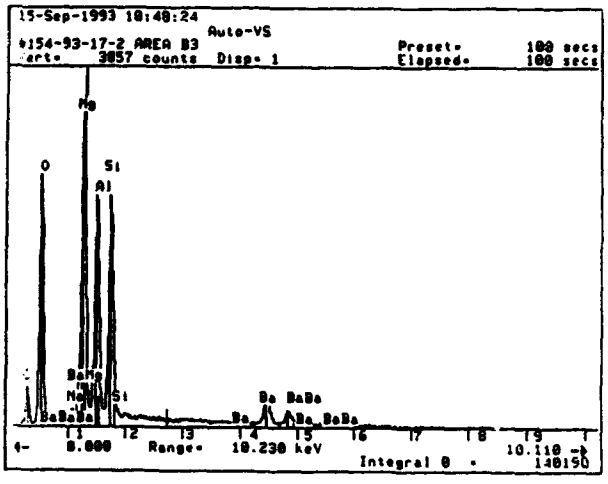

Area 3

Fig. 7 Electron Microbe Analysis of the Surface of BMAS Matrix/SiC/BN Coated Nicalon Fiber Composite #154-93 (1100°C, 100 hrs, O_2, Na_2SO_4) [Away from Na_2SO_4 Coated Region]

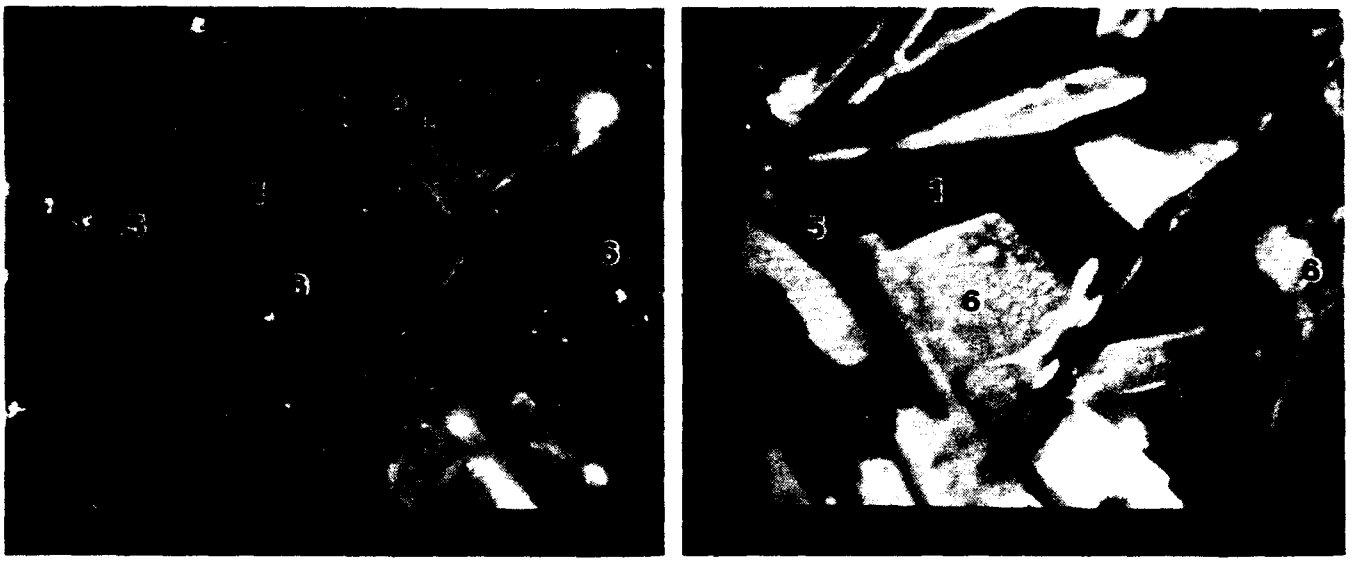

A. SEM

B. BEI

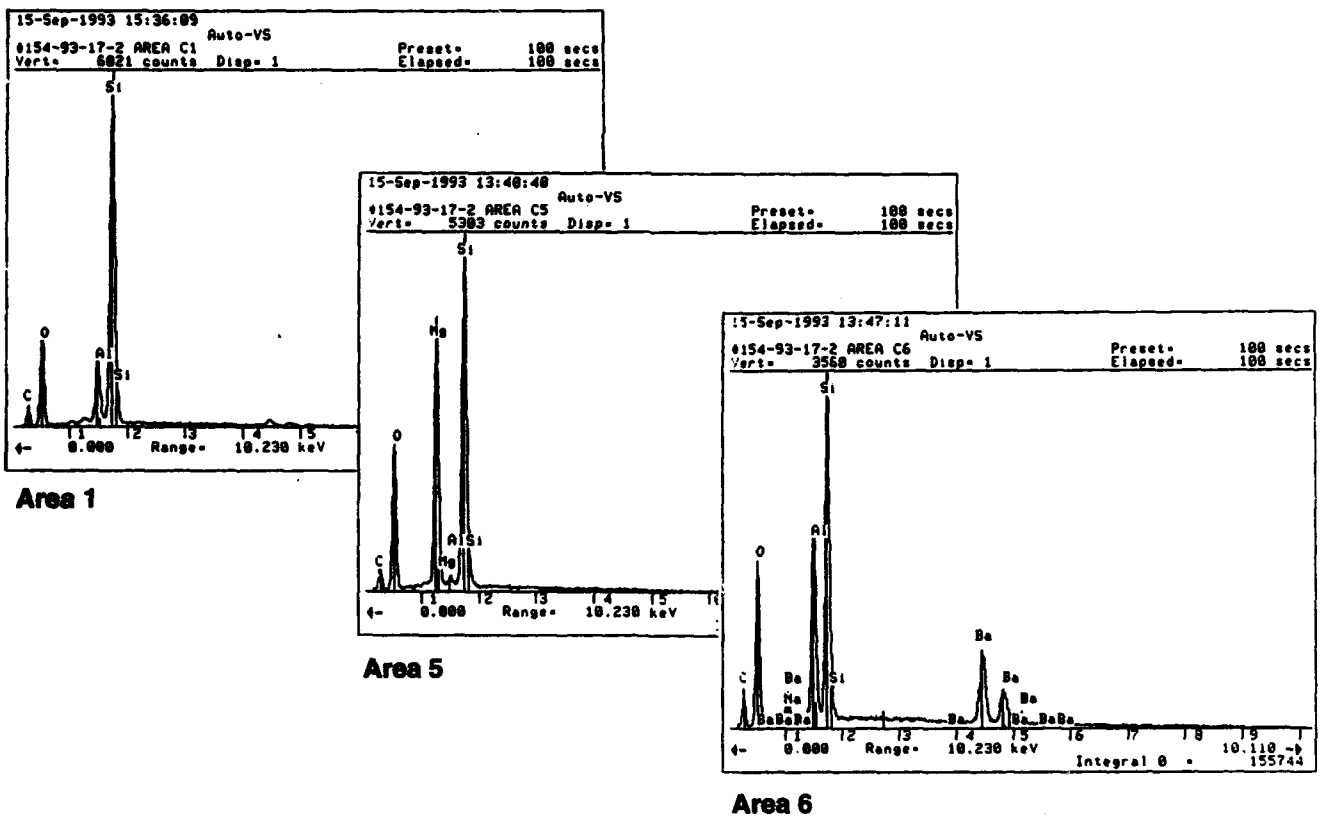

Area 1

Area 5

Area 6

Fig. 8 Electron Microprobe Analysis of the Surface of BMAS Matrix/SiC/BN Coated Nicalon Fiber Composite #154-93 (1100°C, 100 hrs, O_2, Na_2SO_4)

PG232.9

Fig. 9 **Scanning Auger Elemental Map of the Surface of BMAS Matrix/SiC/BN Coated Nicalon Fiber Composite #154-93 After 1000°C, 100 hrs, O_2 (Na_2SO_4)**

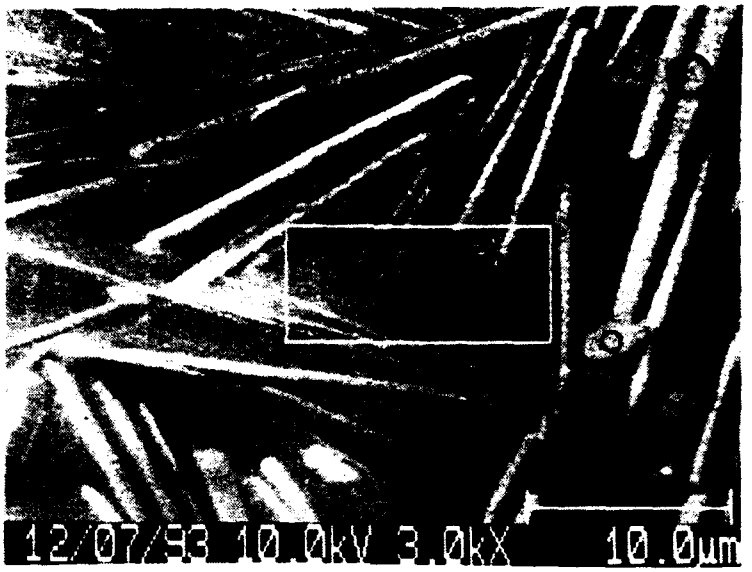

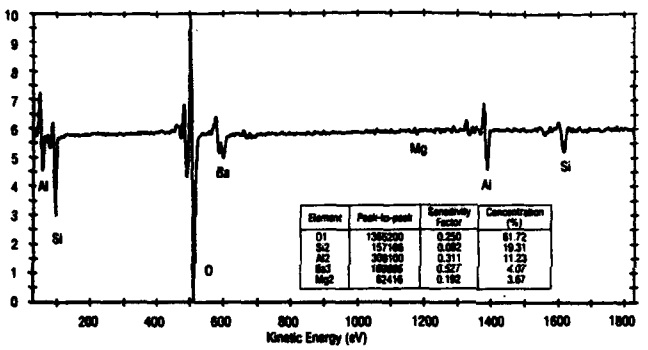

A. Large Circle (BMAS)

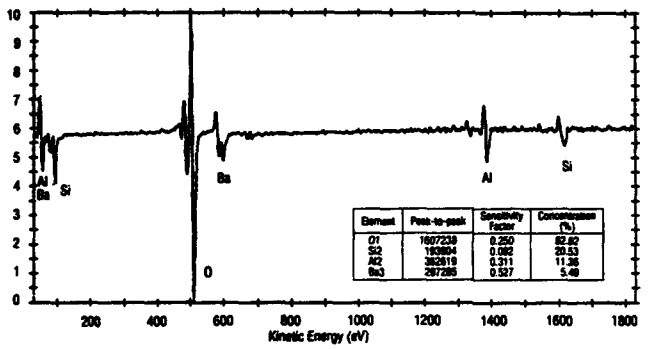

B. Small Circle (BAS)

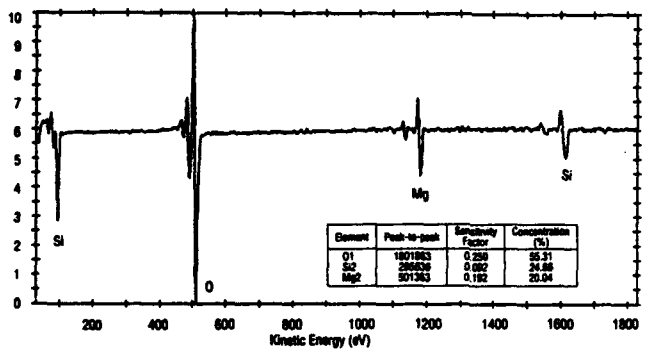

C. Medium Circle (MS)

Fig. 10 Scanning Auger Analysis of the Surface of BMAS Matrix/SiC/BN Coated Nicalon Fiber Composite #154-93 After 1000°C, 100 hrs, O_2 (Na_2SO_4)

PG232.11

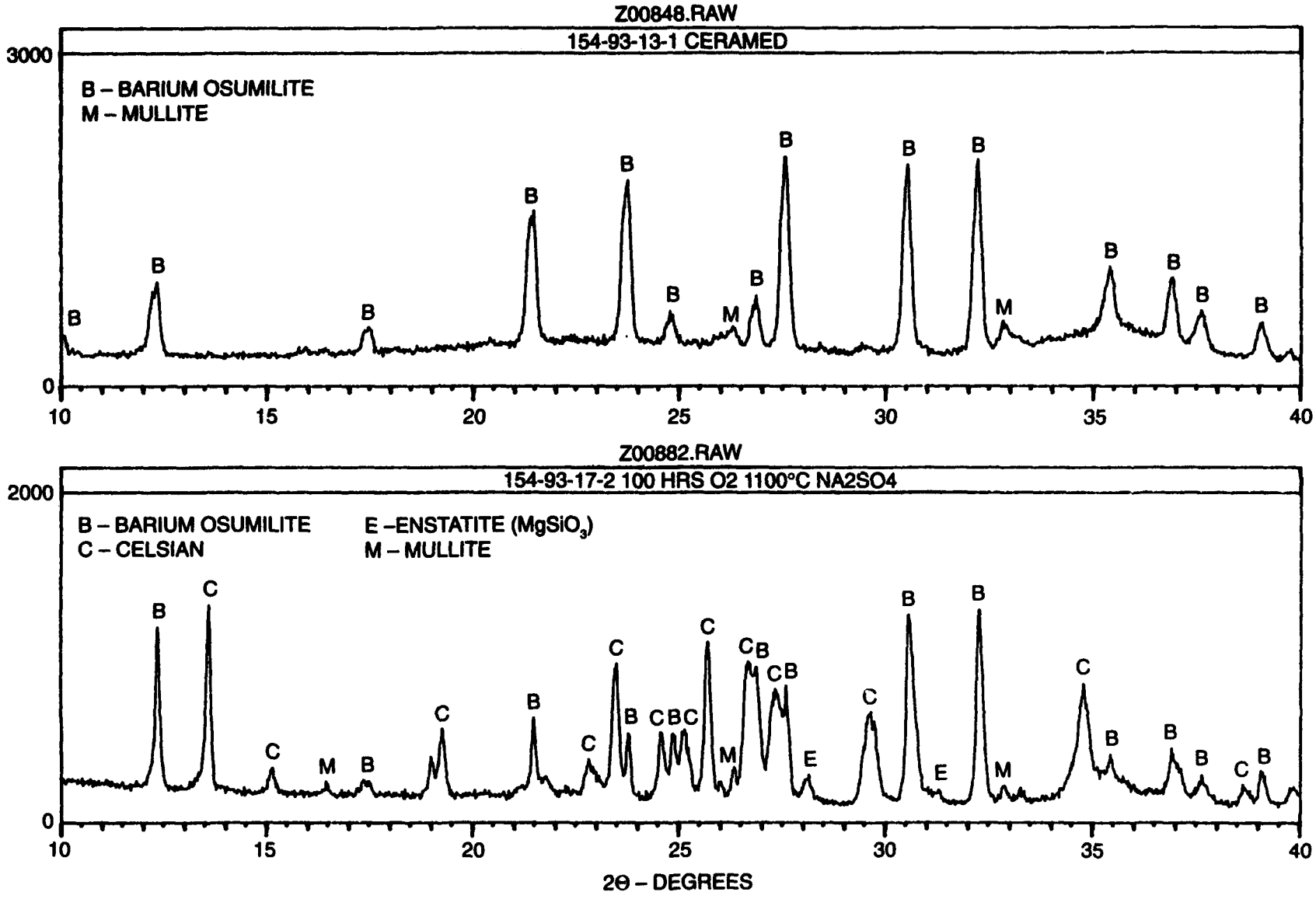

Fig. 11 **X-ray Diffraction Analysis of BMAS Matrix/SIC/ BN Coated Fiber Composite #154-93, As-ceramed (Top) and the Composite Surface After 100 hrs,1100°C, O_2, Na_2SO_4 Coated (Bottom)**

PG232.17

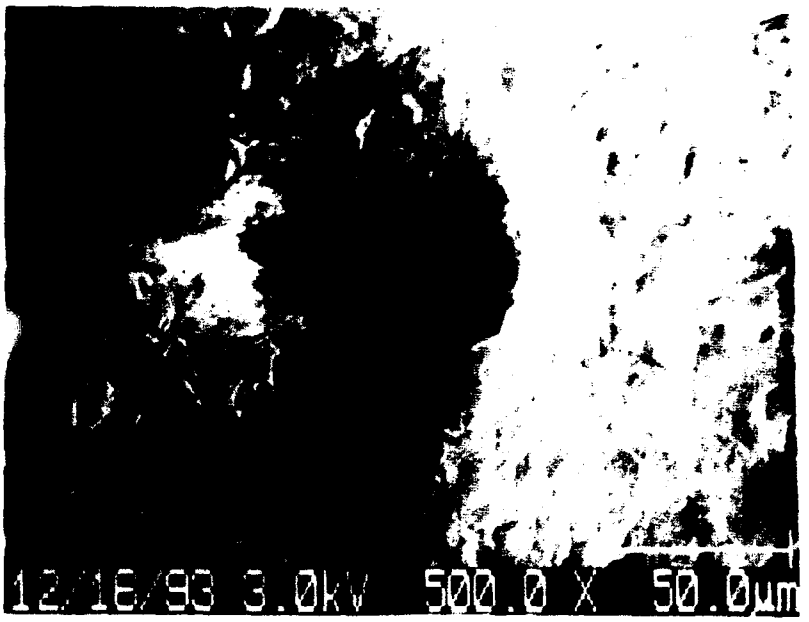

Element	Area (cts-eV/s)	Sensitivity Factor	Concentration (%)
Na1s	21295	1.685	4.54
Ba3d5	24112	7.469	1.16
O1s	129514	0.711	65.40
Si2p	17066	0.378	16.21
Al2p	5204	0.234	7.98
Mg2p	2008	0.153	4.71

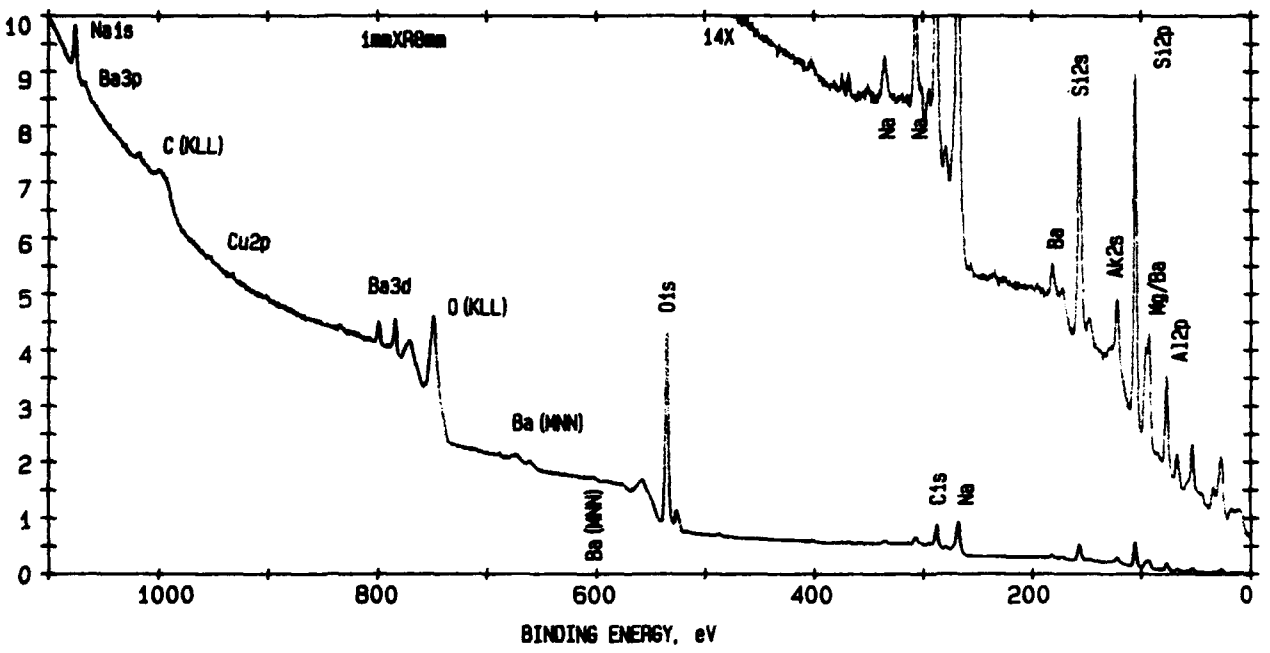

Fig. 12 ESCA Analysis of the Surface of BMAS Matrix/SiC/BN Coated Nicalon Fiber Composite #154-93 After 1000°C, 100 hrs, O_2 (Na_2SO_4)

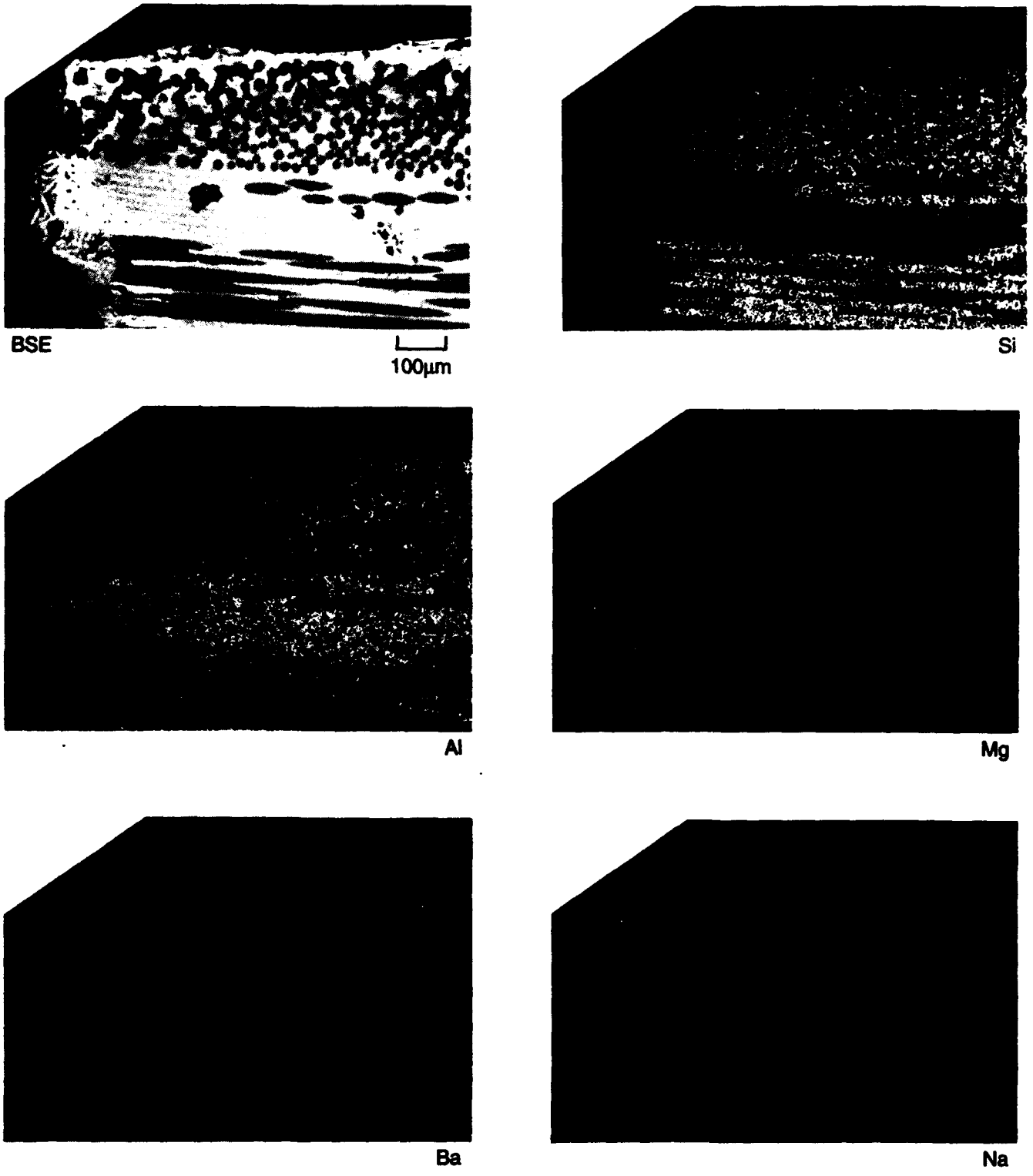

Fig. 13 **Electron Microprobe Elemental Scan of BMAS/SiC/BN/Nicalon Composite #154-93 (Exposed to Na_2SO_4 for 100 hrs, 1100°C, O_2)**

PG232.2

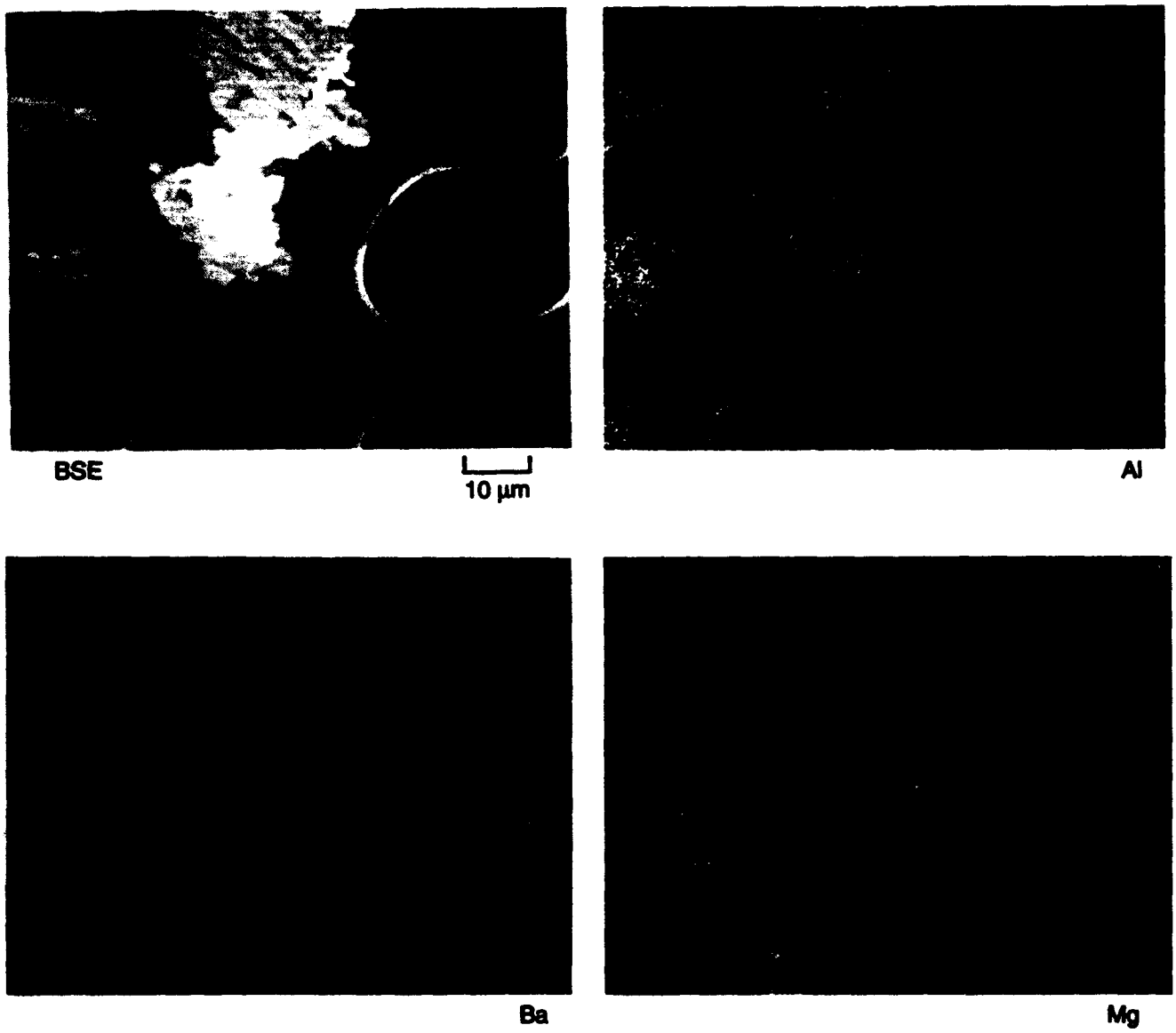

Fig. 14 **Electron Microprobe Elemental Scan of BMAS/SiC/BN/Nicalon Composite #154-93 (Exposed to Na_2SO_4 for 100 hrs, 1100°C, O_2)**

PG232.27

REACTION ZONE NEAR COMPOSITE SURFACE

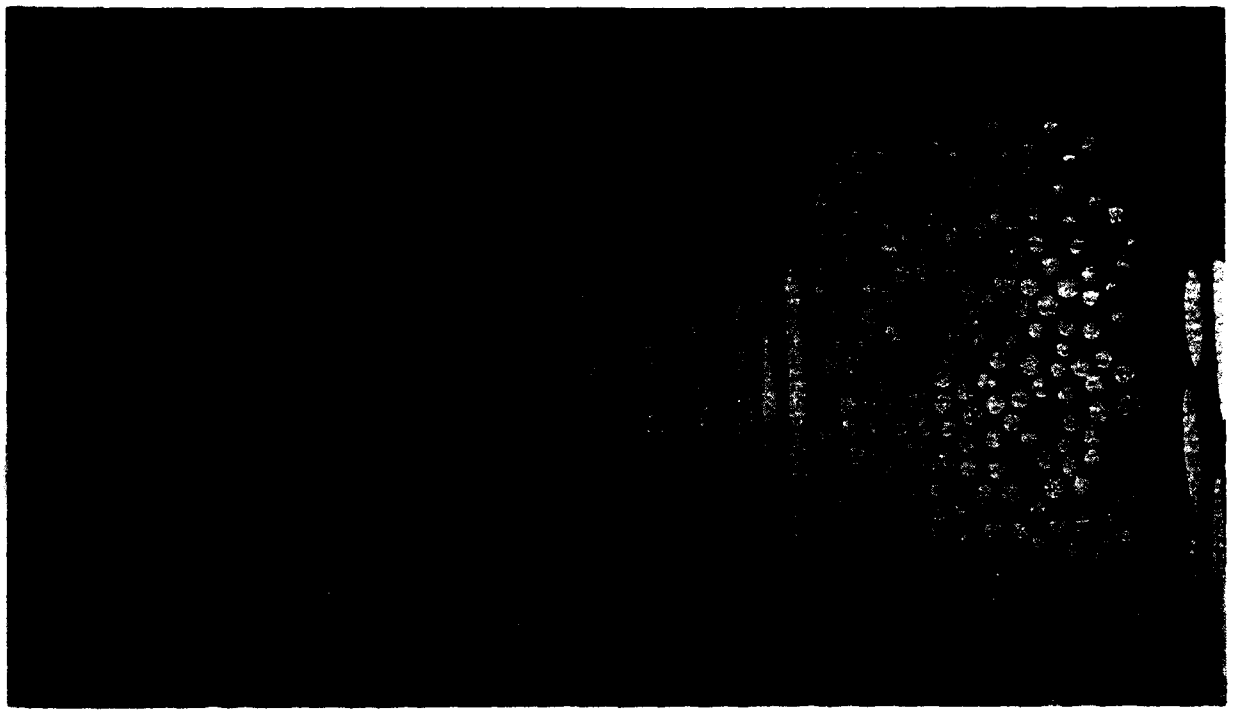

50 μm

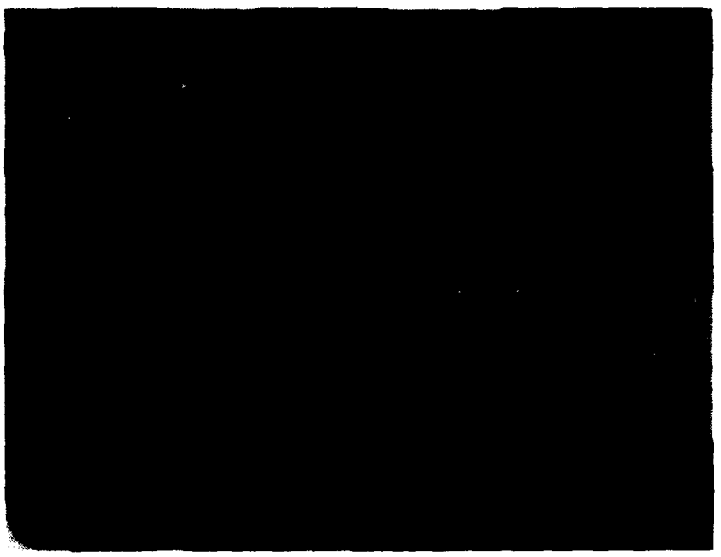

10 μm

Fig. 15 BMAS Matrix/SiC/BN Coated Nicalon Fiber Composite #154-93 (Exposed to Na_2SO_4 for 100 hrs, 1100°C, O_2)

PG232.26

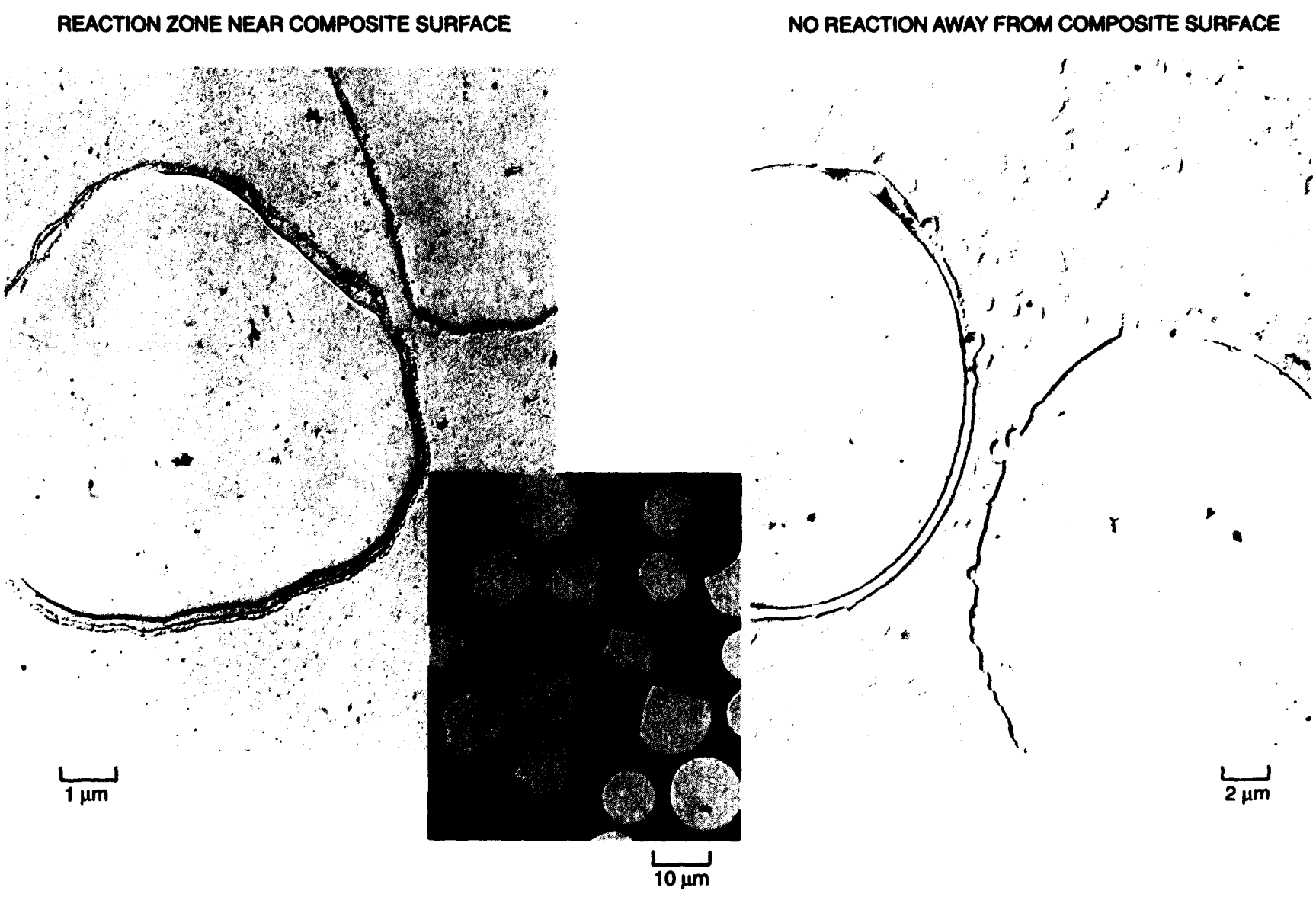

Fig. 16 Optical/TEM Characterization of BMAS/SiC/BN Coated Nicalon Fiber Composite (Exposed to Na_2SO_4, 100 hrs, O_2, 1100°C) #154-93

PG232.19

REACTION ZONE NEAR COMPOSITE SURFACE

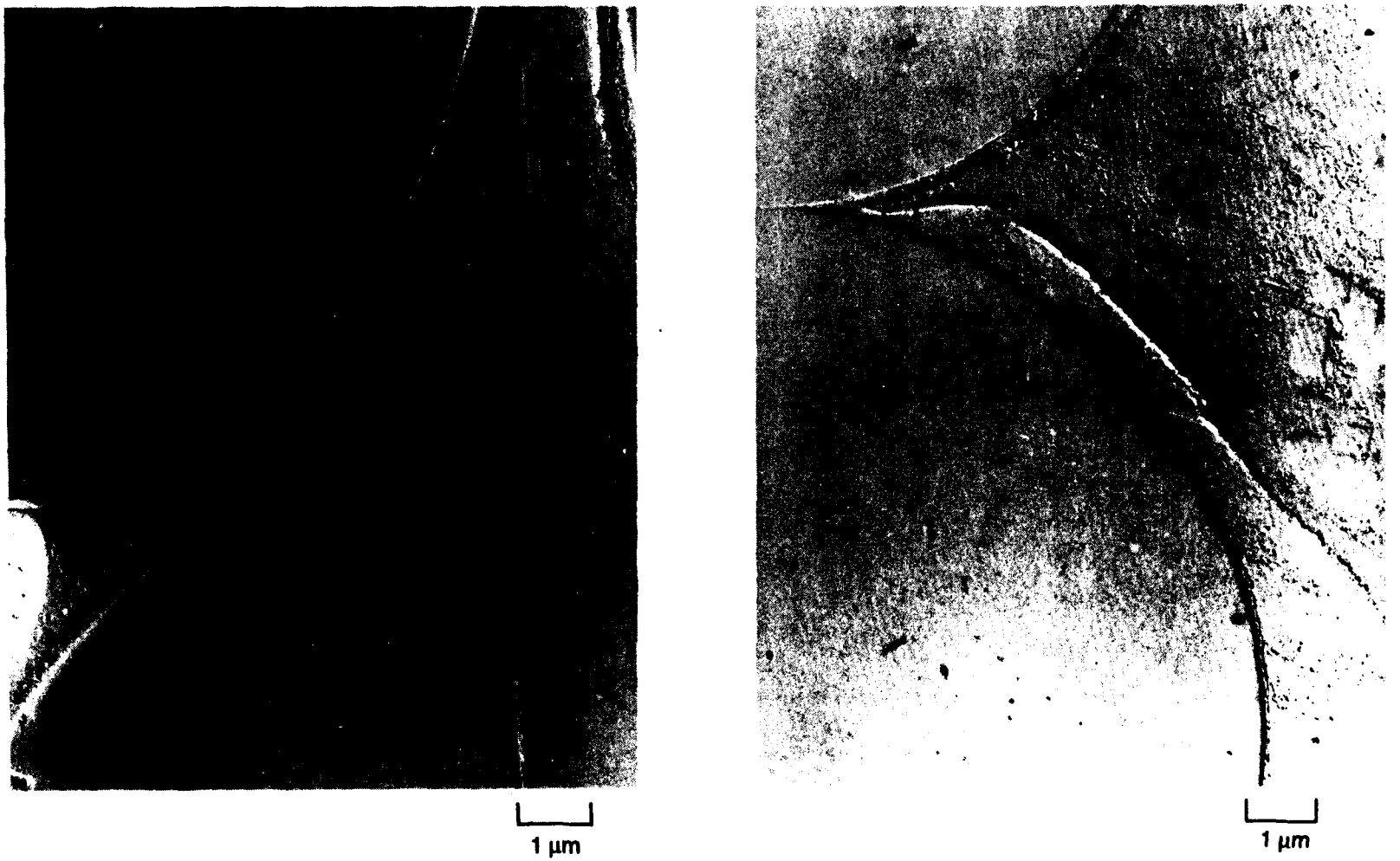

Fig. 17 TEM Characterization of BMAS/SiC/BN Coated Nicalon Fiber Composite (Exposed to Na_2SO_4, 100 hrs, O_2, 1100°C) #154-93

PG232.20

EDGE OF REACTION ZONE, AWAY FROM SURFACE

DARK FIELD IMAGE OF BN COATING

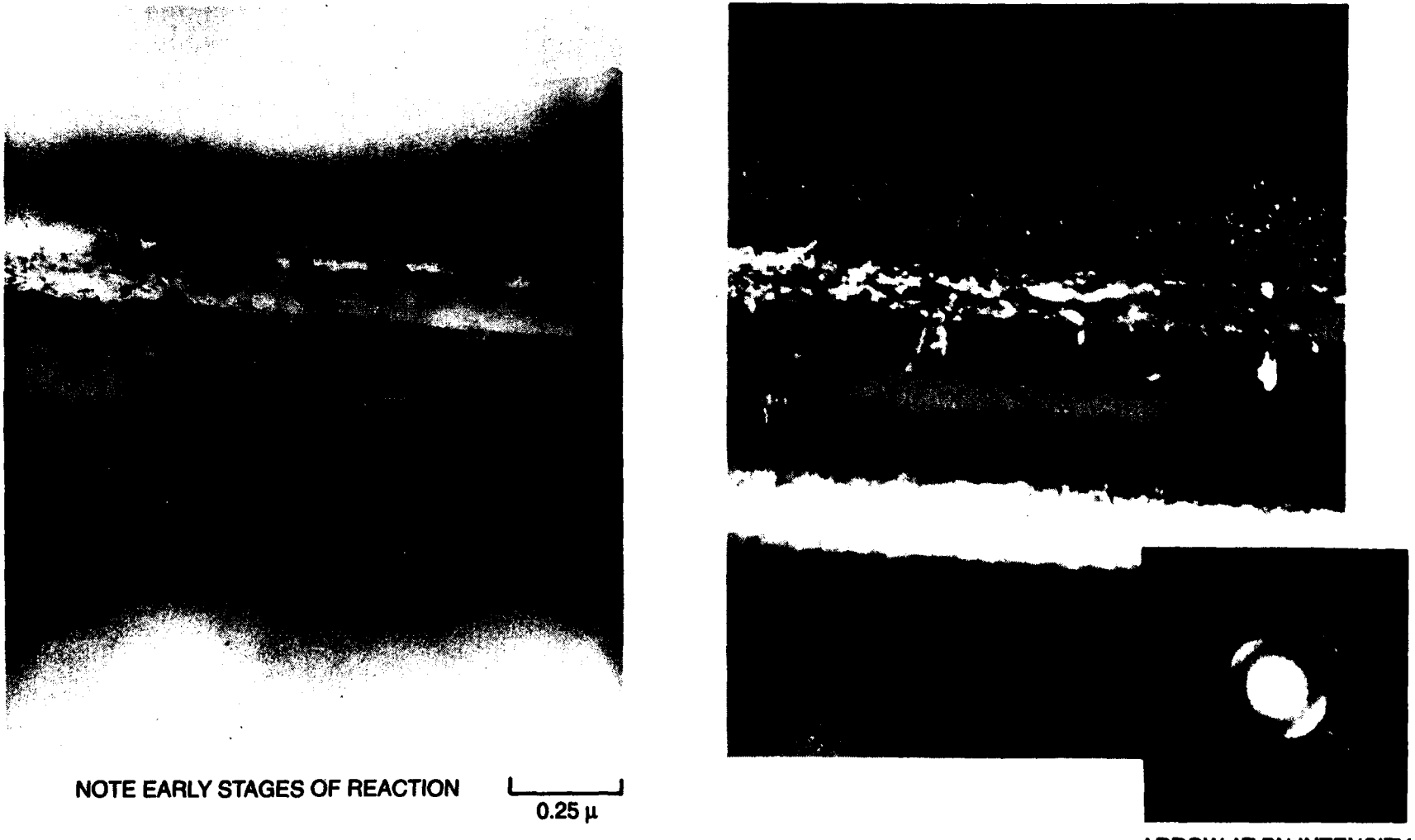

NOTE EARLY STAGES OF REACTION

0.25 μ

ARROW AT BN INTENSITY

Fig. 18 TEM Thin Foil Characterization of BMAS/SiC/BN Coated Nicalon Fiber Composite Exposed to Na_2SO_4 (100 hrs, O_2, 1100°C) #154-93-17-2

PG232.18

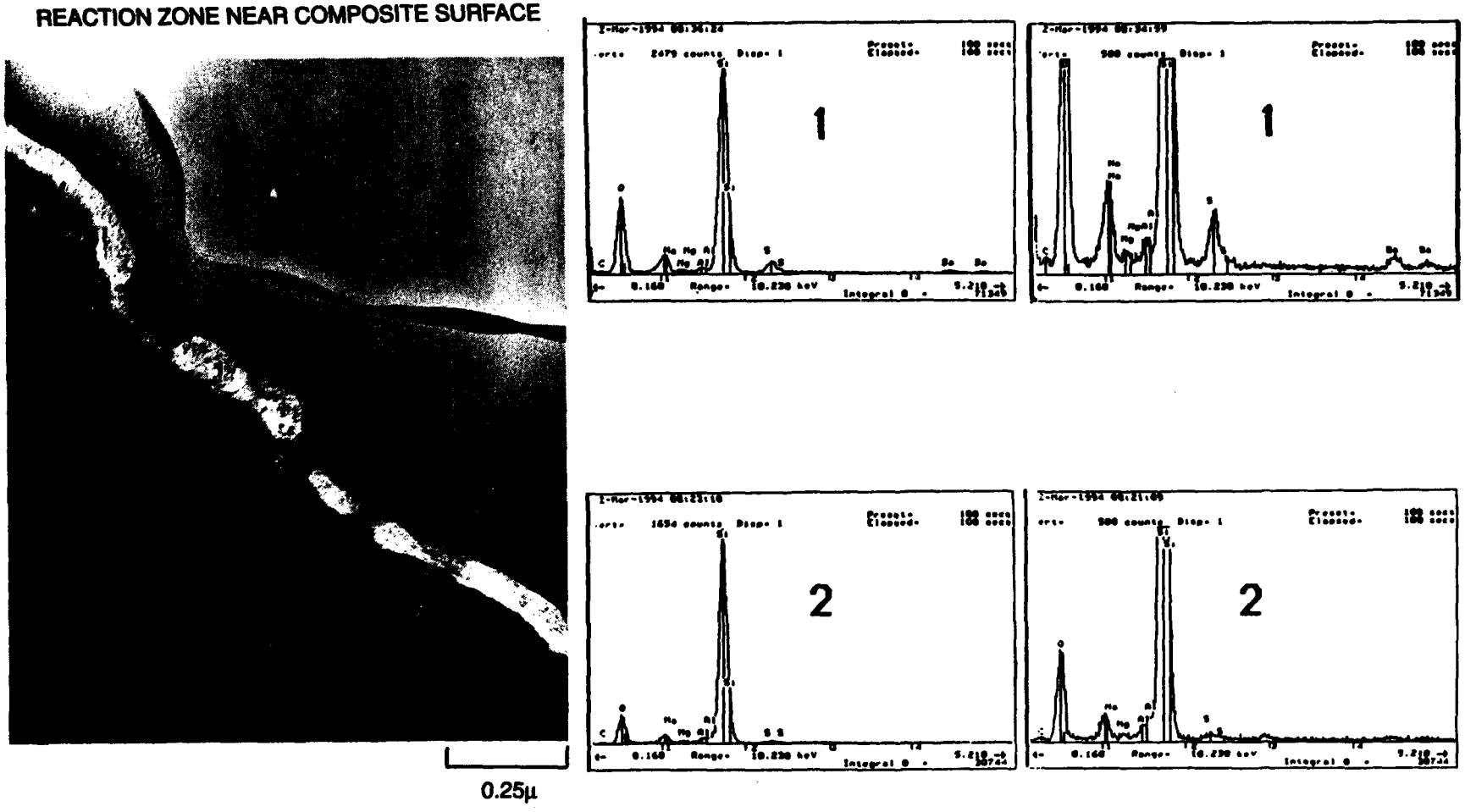

Fig. 19 TEM/EDX Thin Foil Characterization of BMAS/SiC/BN Coated Nicalon Fiber Composite Exposed to Na_2SO_4 (100 hrs, O_2, 1100°C) #154-93-17-2

PG232.21

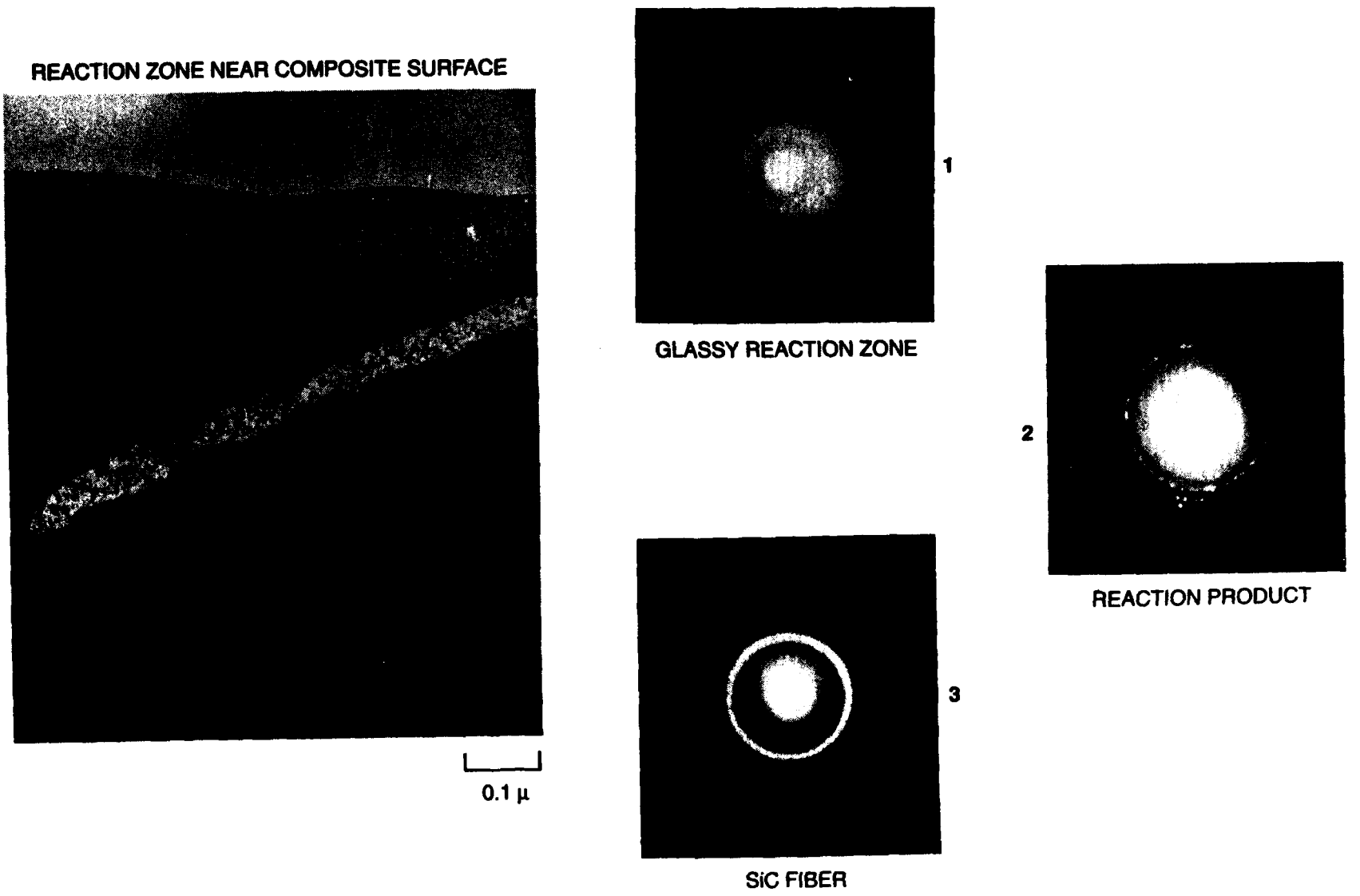

Fig. 20 **TEM/SAED Thin Foil Characterization of BMAS/SiC/BN Coated Nicalon Fiber Composite Exposed to Na_2SO_4 (100 hrs, O_2, 1100°C) #154-93-17-2**

PG232.22

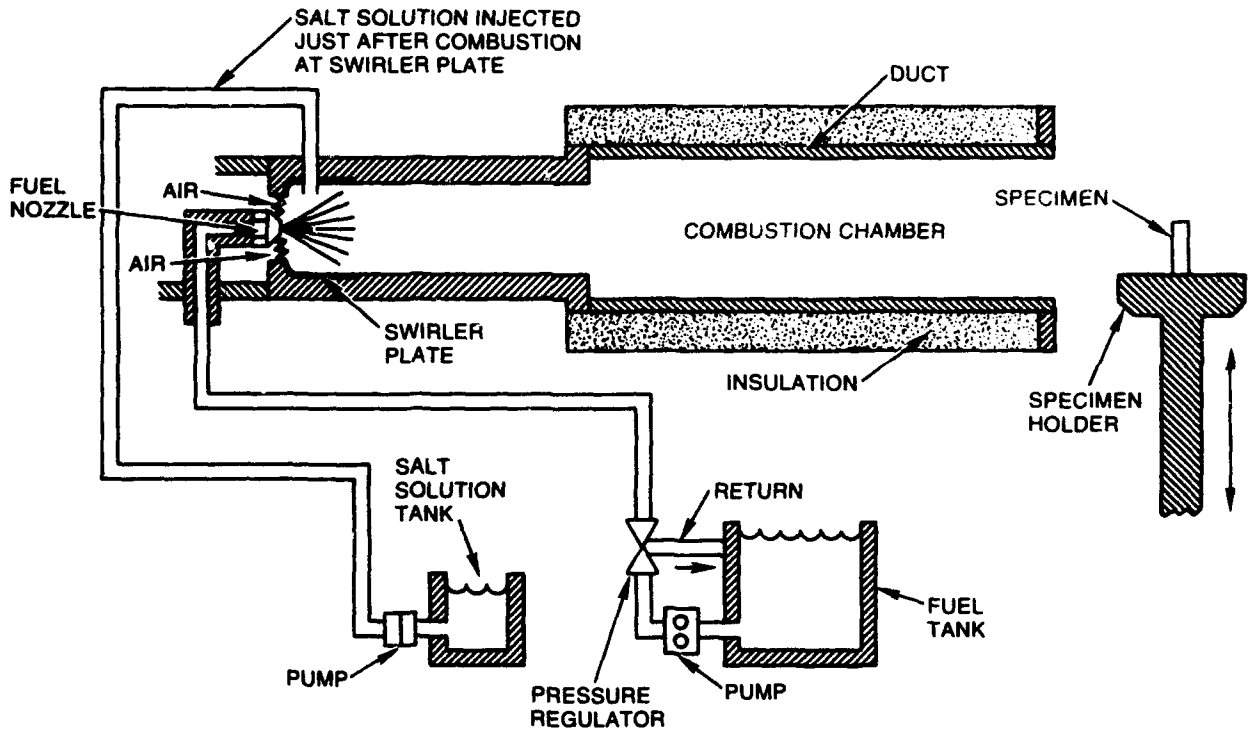

Fig. 21 Schematic of P&W Ducted Burner Rig With Salt Injection

PG232.30

BURNS JET ENGINE FUEL, GAS VELOCITY OF MACH 0.7, VIBRATION AND
EROSION ACTIONS SIMULATE GAS TURBINE ENGINE ENVIRONMENT

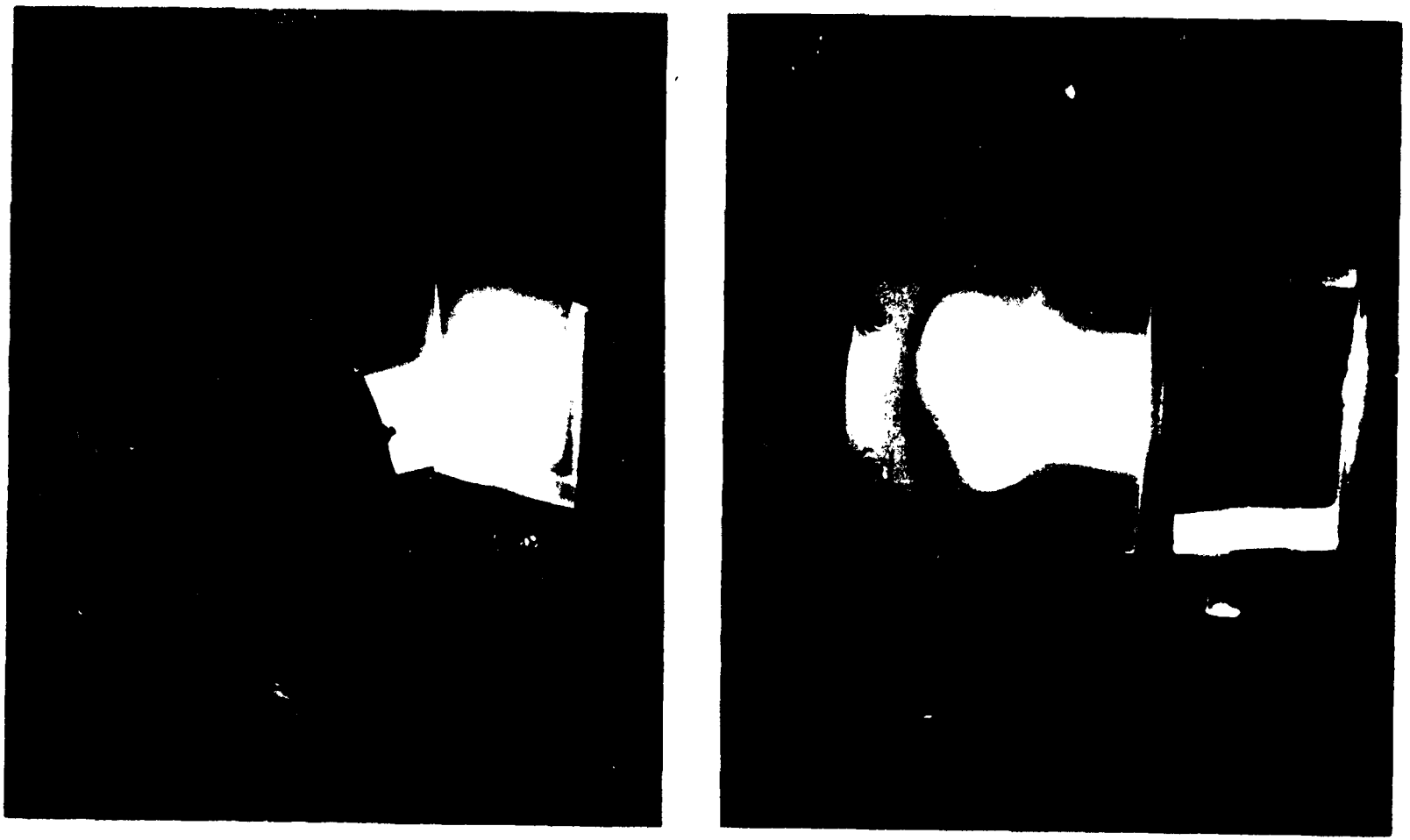

Fig. 22 Pratt & Whitney Impingement Burner Rig

PG232.29

A. Front (Hot) Side

B. Ultrasonic NDE Analysis of Composite #135-92 Before (a) and After (b) 1100°C Burner Rig Test (25 MHz)

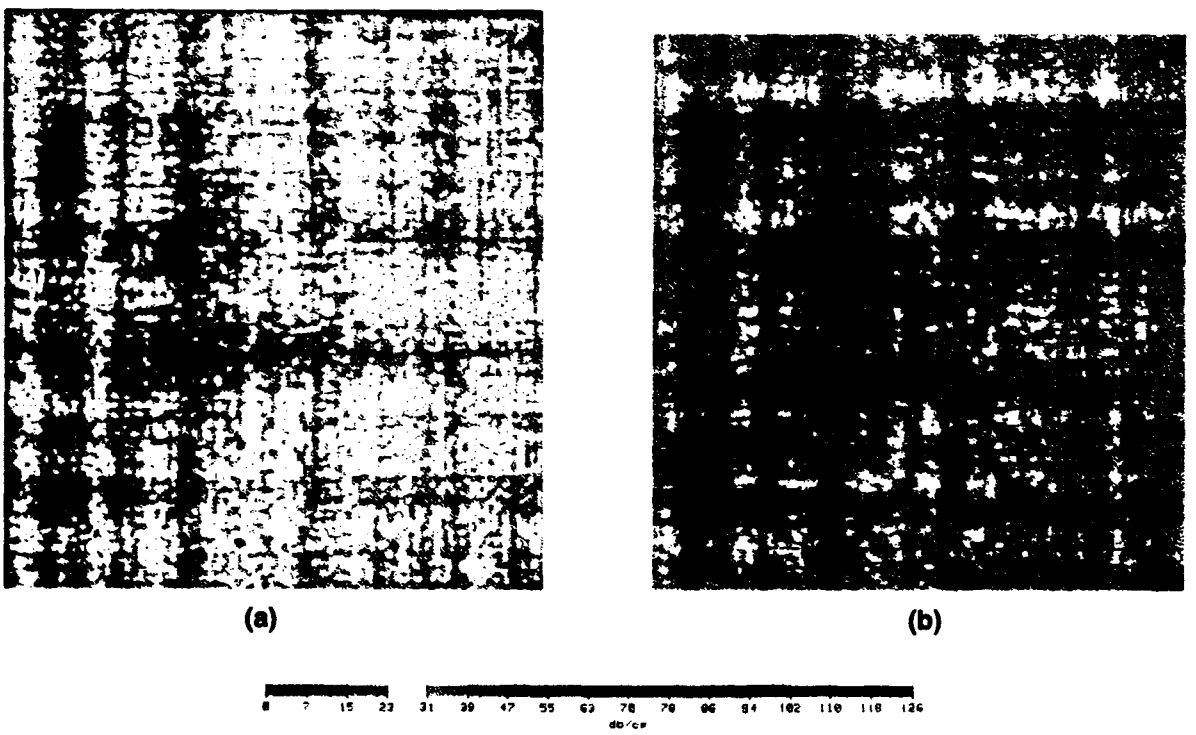

Fig. 23 BMAS Matrix/SiC/BN Coated Nicalon Fiber Composite #135-92 After 1100°C, 6000 Cycle Burner Rig Test (No Sea Salt)

PG232.13

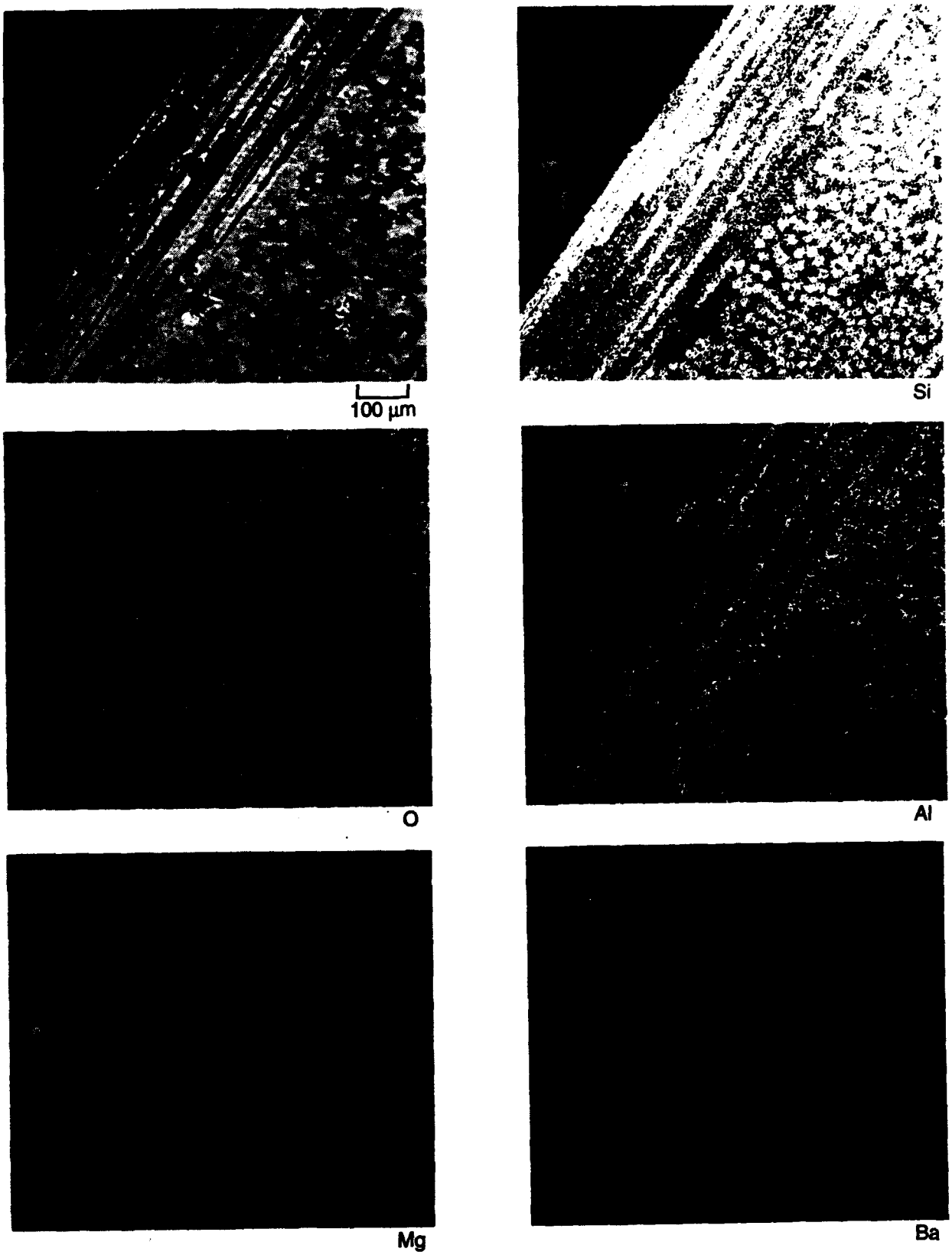

Fig. 24 **BMAS Matrix/SiC/BN Nicalon Fiber Composite #135-92 After 1100°C, 6000 Cycle Burner Rig Test (No Sea Salt)**

PG232.6

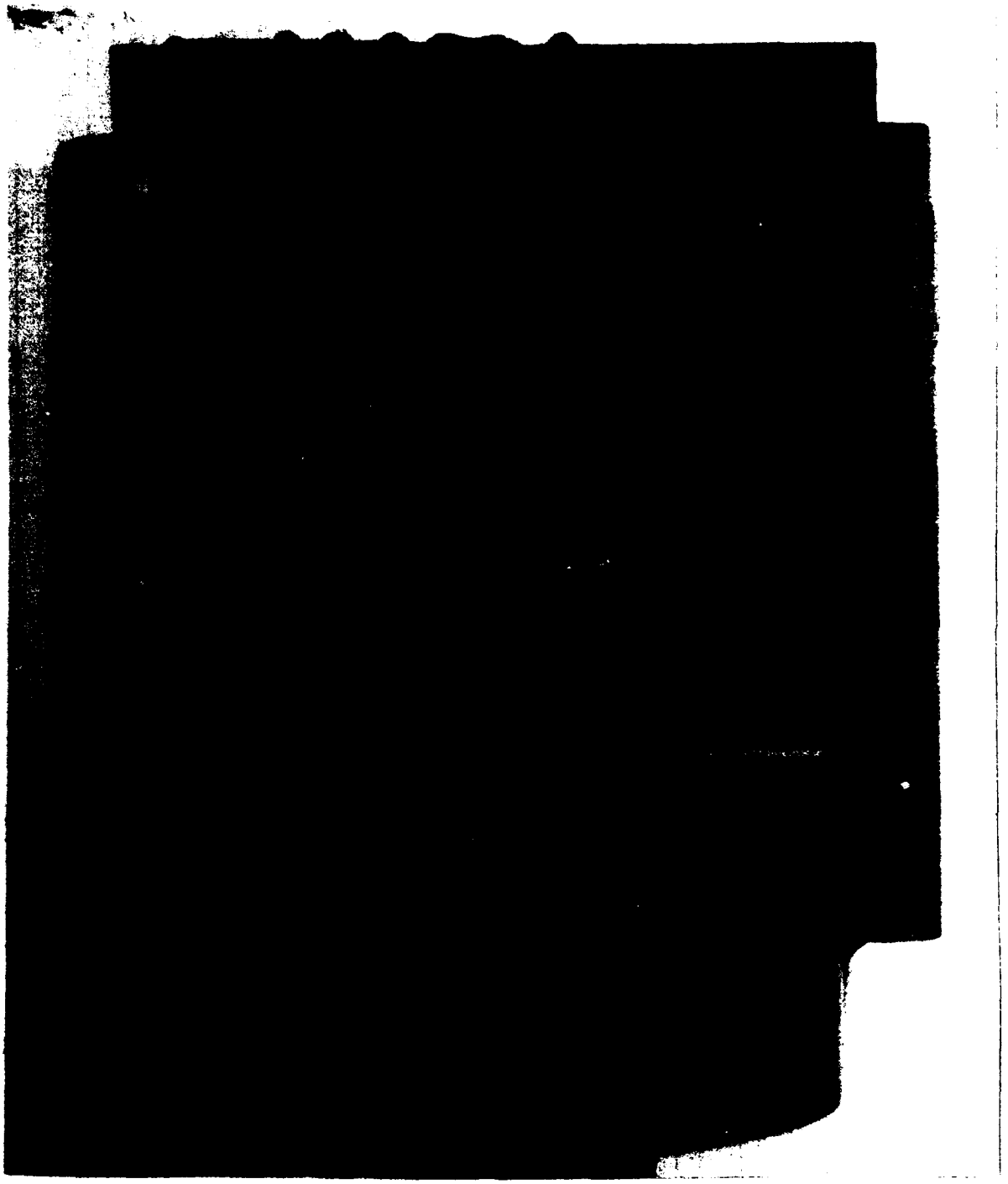

Fig. 25 **BMAS Matrix/SiC/BN Coated Nicalon Fiber Composite #211-93 After 1100°C, 3000 Cycle Burner Rig Test (5ppm Sea Salt Added to Flame)**

PG232.25

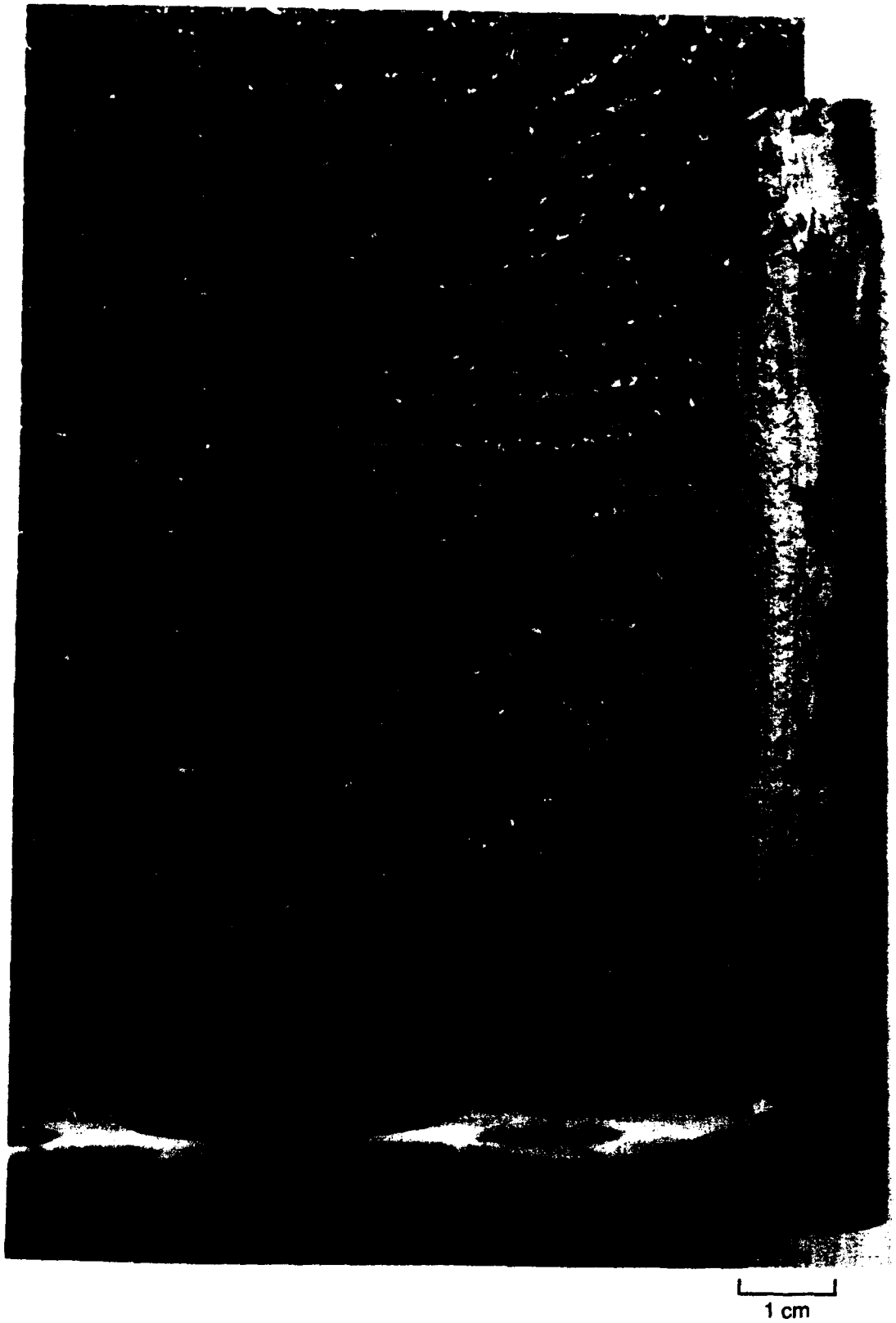

Fig. 26 BMAS Matrix/SiC/BN Coated Nicalon Fiber Composite #211-93 and PWA 1480 Nickel Based Superalloy Posts After 1100°C, 3000 Cycle Burner Rig Test (5ppm Sea Salt Added to Flame)

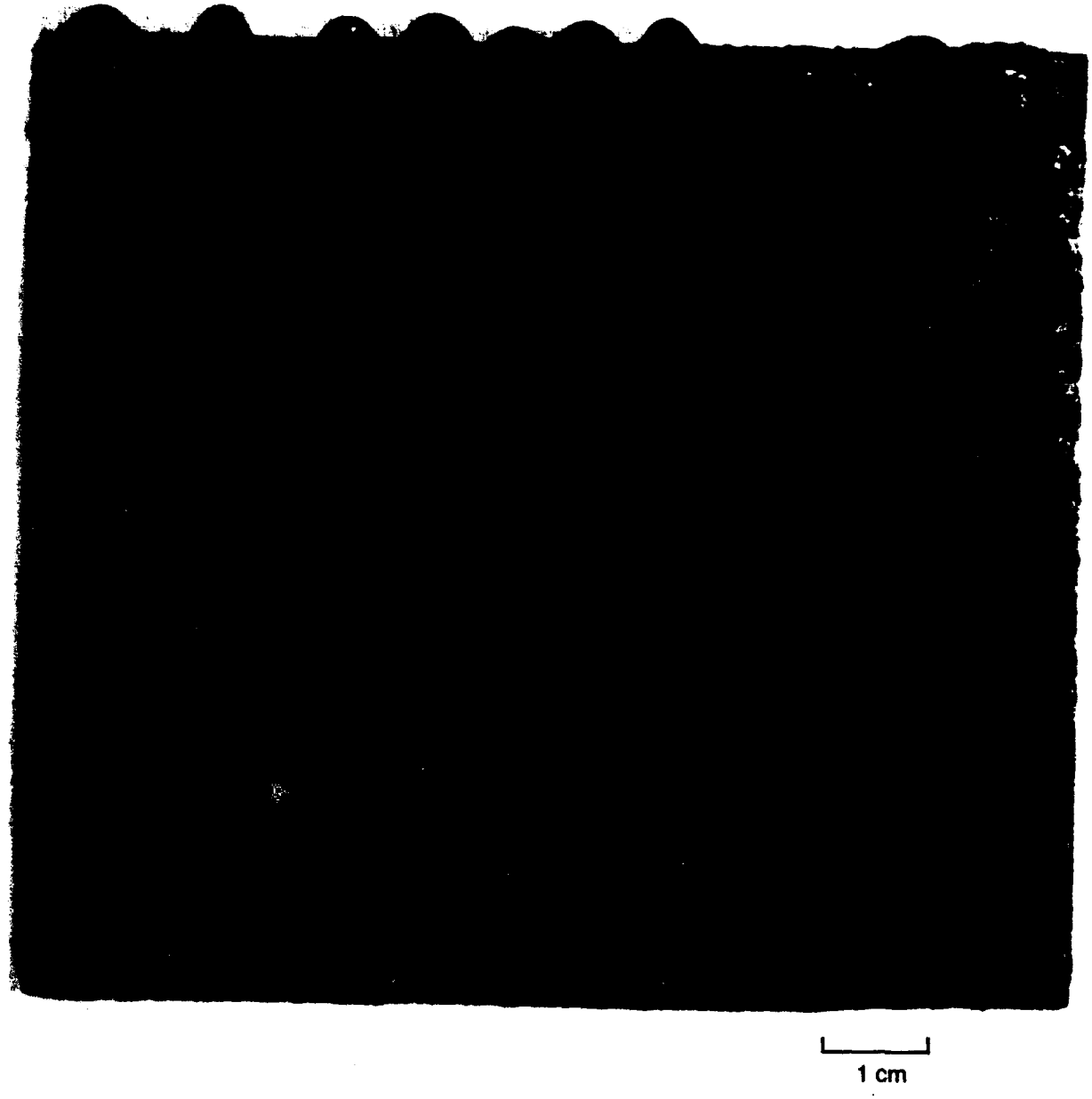

Fig. 27 **BMAS Matrix SiC/BN Coated Nicalon Fiber Composite #211-93 After 1100°C, 6000 Cycle (~100 hrs) Burner Rig Test (5ppm Sea Salt Added to Flame)**

PG232.16

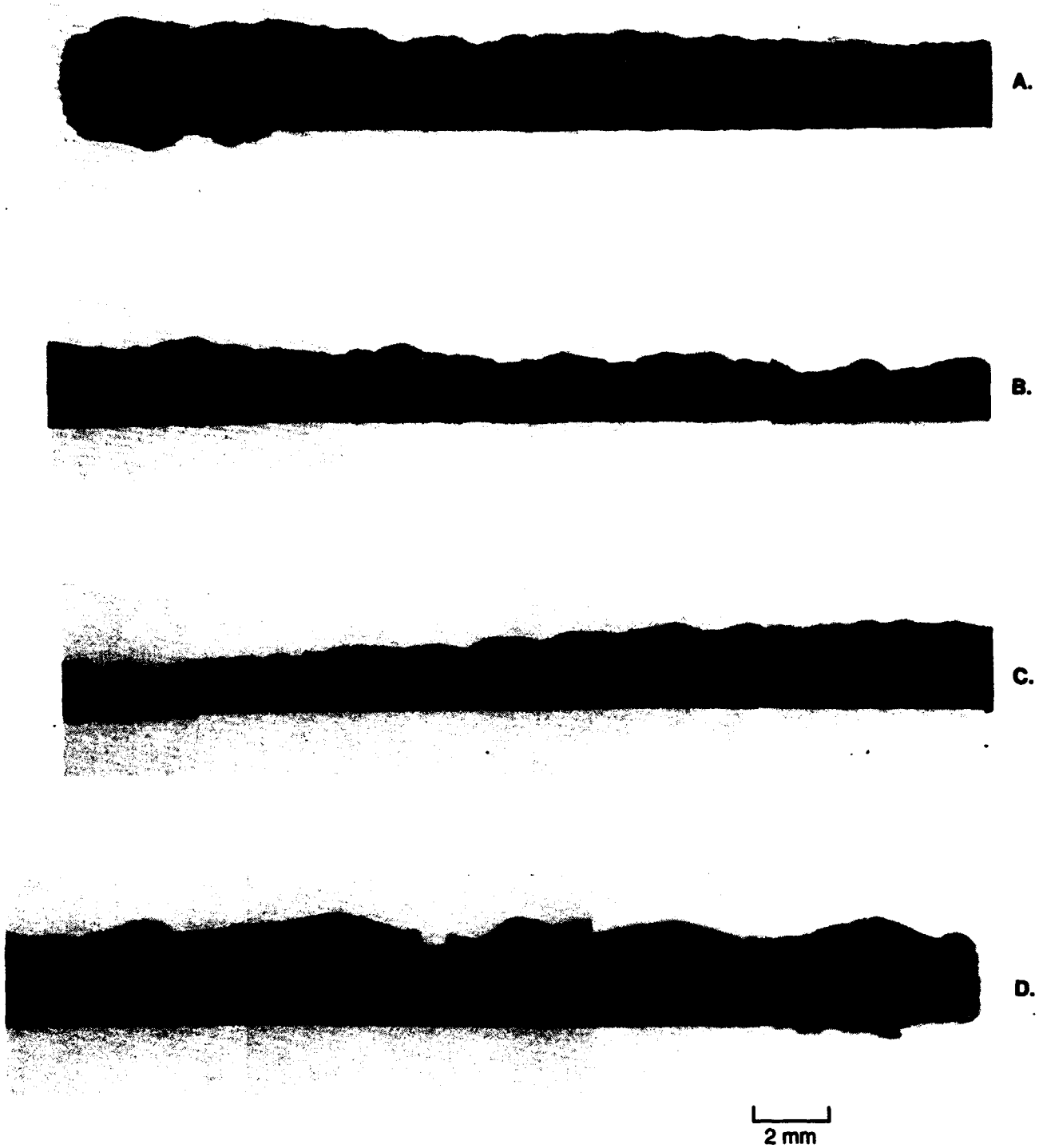

Fig. 28 Cross-section of BMAS Matrix/SiC/BN Coated Nicalon Fiber Composite #211-93 After 1100°C, 6000 Cycle Burner Rig Test (5ppm Sea Salt Added to Flame)

PG232.1

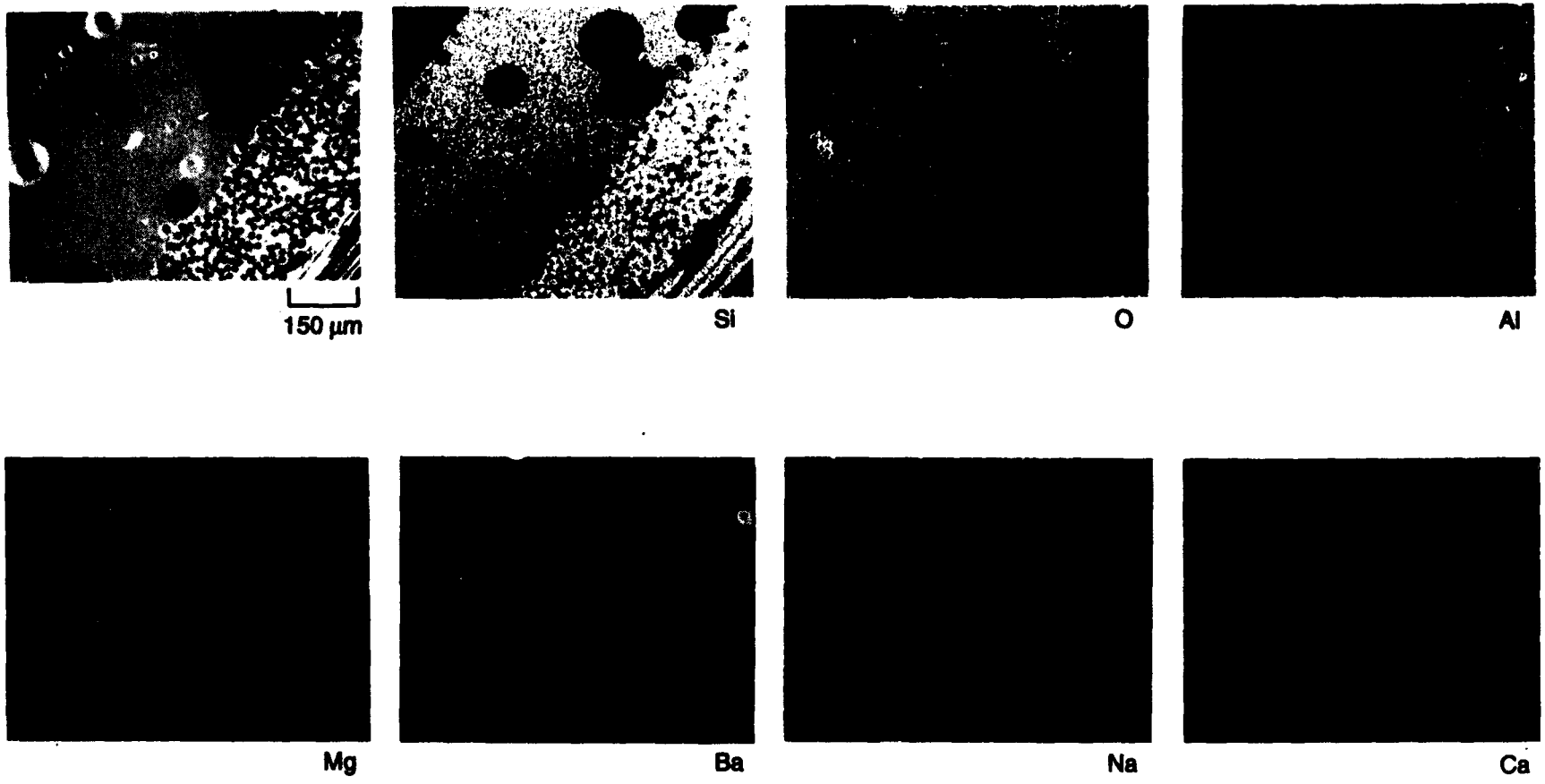

Fig. 29 BMAS/SiC/BN/Nicalon Fiber Composite #211-93 After 1100°C, 6000 Cycle Burner Rig Test With Sea Salt Added to Flame (Edge of Panel)

PG232.24

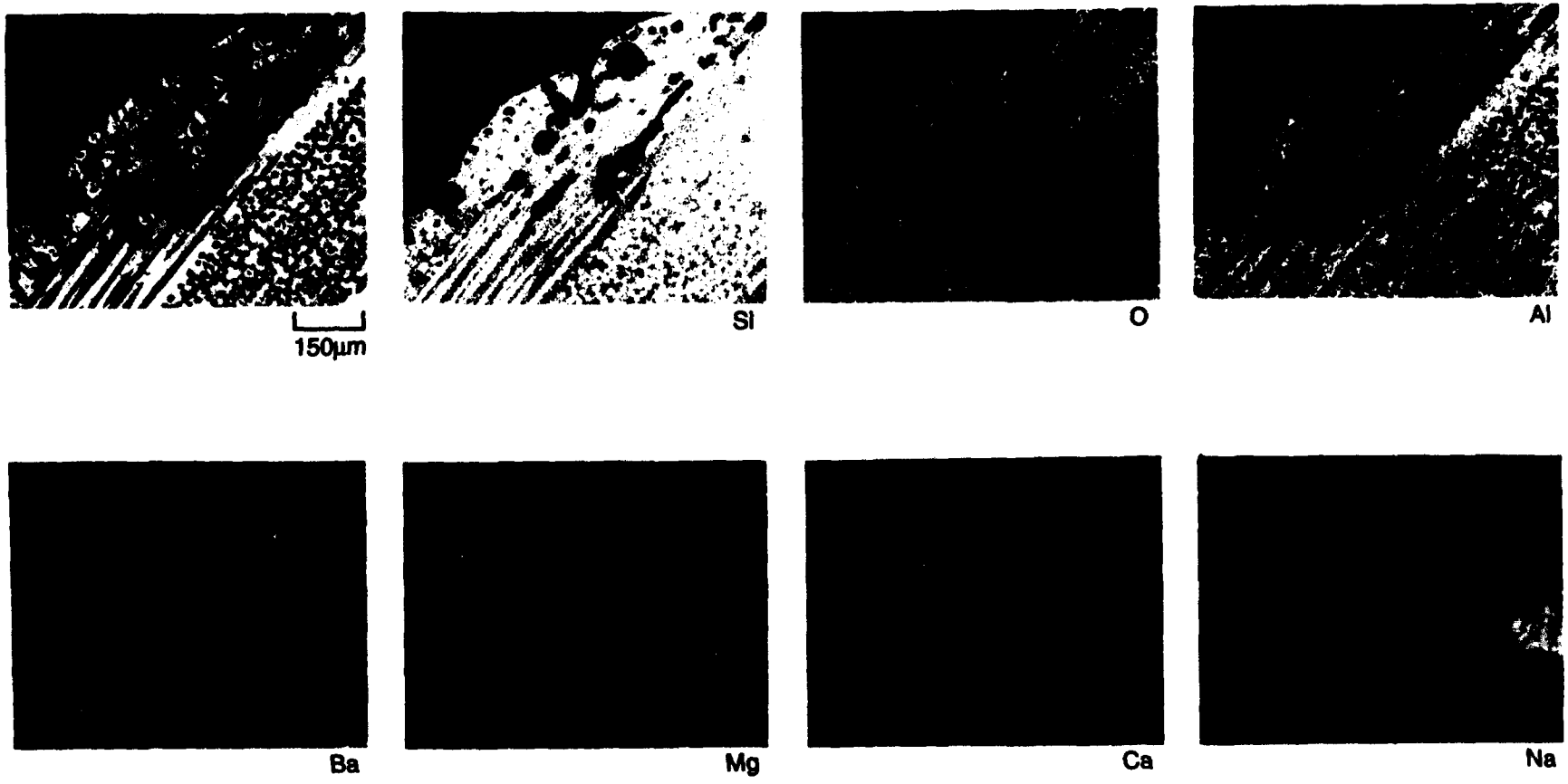

Fig. 30 BMAS/SiC/BN/Nicalon Fiber Composite #211-93 After 1100°C, 6000 Cycle Burner Rig Test With Sea Salt Added to Flame (Center of Panel)

PG232.23